

THREE-DIMENSIONAL NUMERICAL STUDY FOR HEPATIC TUMOR ABLATION USING ELECTRIC CURRENT AND BIOHEAT TRANSFER

By

SAIMA AKTER SAWMPA

Student No. 0419092510

Registration No. 0419092510, Session: April 2019

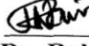
MASTER OF SCIENCE
IN
MATHEMATICS

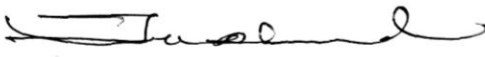


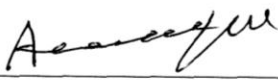
Department of Mathematics
Bangladesh University of Engineering and Technology (BUET)
Dhaka-1000
July, 2021


The thesis titled “**THREE-DIMENSIONAL NUMERICAL STUDY FOR HEPATIC TUMOR ABLATION USING ELECTRIC CURRENT AND BIOHEAT TRANSFER**” Submitted by SAIMA AKTER SAWMPA student no. 0419092510, registration no. 0419092510, session: April 2019, a full-time student of M. Sc. Mathematics has been accepted as satisfactory in partial fulfillment for the degree of Master of Science in mathematics on 12th July 2021.

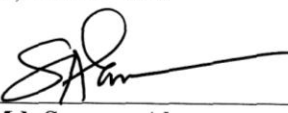
Board of Examiners

1. 

Dr. Rehena Nasrin
Professor
Department of Mathematics
BUET, Dhaka-1000
Chairman
(Supervisor)
2. 

Dr. Khandker Farid Uddin Ahmed
Headand Professor (Ex-Officio)
Department of Mathematics
BUET, Dhaka-1000
Member
3. 

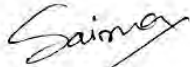
Dr. Md. Abdul Maleque
Professor
Department of Mathematics
BUET, Dhaka-1000
Member
4. 

Dr. Nazma Parveen
Professor
Department of Mathematics
BUET, Dhaka-1000
Member
5. 

Dr. Md. Sarwar Alam
Professor
Department of Mathematics
Jagannath University, Dhaka-1100
Member
(External)

Author's Declaration

I hereby announce that the work which is being presented in this thesis entitled **“THREE DIMENSIONAL NUMERICAL STUDY FOR HEPATIC TUMOR ABLATION USING ELECTRIC CURRENT AND BIOHEAT TRANSFER”** submitted in partial fulfillment of the requirements for the declaration of the degree of Master of Science, Department of Mathematics, BUET, Dhaka, is an authentic record of my work. The work is also original except where indicated by and attached with special reference in the context and no part of it has been submitted for any attempt to get other degrees or diplomas. I authorize the Bangladesh University of Engineering and Technology to lend this thesis to other institutions or individuals for scholarly research.




(SAIMA AKTER SAWMPA)
Date: 12th July, 2021

Dedicated to

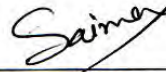
My Parents & Teachers

Permit of Research

This is to endorse that the work presented in this thesis is carried out by the author under the supervision of Dr. Rehana Nasrin, Professor, Department of Mathematics, Bangladesh University of Engineering and Technology (BUET), Dhaka-1000, Bangladesh.

 12/7/21

Dr. Rehana Nasrin
Professor
Dept. of Mathematics
BUET, Dhaka-1000



SAIMA AKTER SAWMPA

Acknowledgment

I would like to affirm the notable recognizance of Almighty's continual mercy because no work would have been possible to accomplish the goal line without the help of Allah. With great pleasure, I take this opportunity to place on the record of deepest respect and sincerest gratitude to my Supervisor Professor Dr. Rehena Nasrin, Department of Mathematics, Bangladesh University of Engineering and Technology, Dhaka for her expert guidance and valuable suggestions throughout this work. It would not have been possible to carry out this study successfully without continuous inspiration, guidance, constant support, intuitive suggestions, and relentless encouragement from the supervisor.

I owe a favor to Dr. Khandker Farid Uddin Ahmed, Professor, and Head of, Department of Mathematics, Bangladesh University of Engineering and Technology, for his support in allowing me to use the departmental facilities in various stages of my work.

I am also deeply indebted to Professor Dr. Md. Abdul Maleque and Professor Dr. Nazma Parveen, Department of Mathematics, BUET for their wise and liberal co-operation in providing me all necessary help from the department during my course of M.Sc. Degree. I wish to thank all staff of the Department of Mathematics, Bangladesh University of Engineering and Technology, for their cooperation in this work.

I would like to take the opportunity to thank the external member of the Board of Examiners for my thesis. I am grateful to him for his valuable suggestions to improve this thesis work.

Finally, I would like to express my gratitude to my dear mother and father for their steadfast love and support. They have kept me going through the most difficult times.

Abstract

In this research, the finite-element method (FEM) analysis has been employed in the determination of the distribution of tissue temperature during radiofrequency hepatic tumor ablation. We have investigated three-dimensional (3D) thermal-electric FEM including a four-tine RF probe, hepatic tissue, and an integrated model of a large blood vessel (10-mm diameter). We simulated our FEM analyzes under temperature-controlled (90°C) 10-minutes ablation. Though the heated targeted cells are supposed to kill and the healthy surrounding tissues are supposed to save. Using the COMSOL Multiphysics software, we have numerically replicated the ablation process. The finite element method of Galerkin's weighted residual is employed to solve the governing system of equations (electric current and Bioheat equations) with proper boundary conditions. The numerical simulation has been conducted various times from 0 to 600 s and electric voltage from 22 to 50 V with good convergence of the iterative scheme. In the term of temperature fields at different times, Iso-surfaces with temperatures of 50°C at various times, Iso-surfaces at different temperatures, and the temperature distribution over time are displayed. Temperature distribution versus time at the tip of one of the electrodes arm at a fixed voltage and various voltages has displayed graphically. Results from the RF simulation indicate that temperature increases due to increasing time of ablation of tumor and electric voltage. The tumor cell has killed approximately at 50°C with 22 V after 480 s heating. The proposed model could be a new tool for physicians for the efficient thermal insulation of tumors without any significant damage in healthy tissues.

Table of Contents

Board of Examiners	Error! Bookmark not defined.
Author’s Declaration	Error! Bookmark not defined.
Permit of Research	Error! Bookmark not defined.
Acknowledgment	iv
Abstract	vii
Table of Contents	viii
Nomenclature	x
List of Table	xii
List of Figures	xiii
CHAPTER 1: INTRODUCTION	1
1.1 Overview	1
1.1.1 Malignant tumor	1
1.1.2 Radio-frequency ablation	2
1.1.3 RF probe	3
1.1.4 Bio-heat transfer equation	4
1.1.5 Electric potential	5
1.1.6 Image-guided technique	5
1.2 Literature Review	6
1.3 Motivation	9
1.4 Objectives	9
1.5 Possible Outcomes	9
1.6 Outline of Thesis	10
CHAPTER 2: NUMERICAL TECHNIQUES	11
2.1 Introduction	11
2.2 Advantage of Numerical Analysis	12
2.3 The steps of a Numerical solution	12
2.3.1 Mathematical model	12
2.3.2 Discretization techniques	13

2.3.3 Meshing	13
2.3.4 Accuracy	13
2.3.5 Grid system	13
2.3.6 Solution technique	14
2.4 Finite Element Method.....	14
2.5 Galerkin’s Weighted Residual Technique.....	16
CHAPTER 3: NUMERICAL MODELING OF RF HEPATIC TUMOR ABLATION.....	18
3.1 Introduction.....	18
3.2 Physical Model.....	18
3.3 Governing Equations.....	21
3.4 Solution Procedure.....	23
3.4.1 Mesh generation.....	24
3.4.2 Code validation	25
CHAPTER 4: RESULTS AND DISCUSSIONS	27
4.1 Introduction.....	27
4.2 Effect of Time.....	27
4.3 Effect of Electric Voltage.....	35
4.4 Comparison.....	40
CHAPTER 5: CONCLUSION AND FUTURE RESEARCH	42
5.1 Conclusions.....	42
5.2 Future Research.....	43
REFERENCES.....	44

Nomenclature

C_b	Heat capacity of blood [$\text{Jkg}^{-1}\text{K}^{-1}$]
C_p	Heat capacity at constant pressure [$\text{Jkg}^{-1}\text{K}^{-1}$]
E	Electric field intensity [Vm^{-1}]
J	Current density [Am^{-1}]
T	Temperature [K]
T_0	Initial domain temperature [K]
T_b	Arterial blood temperature [$^{\circ}\text{C}$]
Q_{ext}	Spatial heating [Wm^{-3}]
Q_{met}	Heat sources from metabolism [Wm^{-3}]
Q_j	Current source [Am^{-3}]
V	Electric Voltage [V]

Greek symbol

ρ_b	Blood density [kgm^{-3}]
ω_b	Blood perfusion rate [s^{-1}]
σ	Electrical conductivity [sm^{-1}]
κ	Thermal conductivity [$\text{Wm}^{-1}\text{K}^{-1}$]
ρ	Tissue density [kgm^{-3}]

Abbreviation

AC	Alternating current
CFD	Computational fluid dynamics
CT	Computed tomography
DC	Direct current
MWR	Method of weighted residuals

MR	Magnetic resonance
MRI	Magnetic resonance imaging
RFA	Radiofrequency ablation
RF	Radiofrequency
RFE	Radiofrequency exposure
RITA	Record of in-training assessment

List of Table

Items	Table Caption	Page
Table 3.1	Value of basic blood parameters	23
Table 3.2	Thermal and electrical properties	23
Table 4.1	Comparison of temperature between present numerical research and research of Mellal <i>et al.</i> [9]	41

List of Figures

Items	Figure Caption	Page
Figure 1. 1	Differences between healthy and malignant tissue and malignant tumor in liver	2
Figure 1.2	Radiofrequency ablation of liver	3
Figure 1.3	RF probe with four electrode arm	4
Figure 1.4	CT-guided radiofrequency ablation for liver treatment	6
Figure 2.1	Finite element simulation of liver	16
Figure 3.1	(a) Cylindrical domain with the four-armed electric probe and (b) computational domain	19
Figure 3.2	Fully deployed four-tine probe structure for hepatic tumors	20
Figure 3.3	3D domain (a) external view and (b) internal view	20
Figure 3.4	Finite element meshing of 3D domain	25
Figure 3.5	Element quality histogram	25
Figure 3.6	Code validation of the temperature distribution in liver tissue between Surita <i>et al.</i> [28] and present code	26
Figure 4.1	Temperature fields for various time (i) 60, (ii) 120, (iii) 180, (iv) 360, (v) 420 and (vi) 480 s at 22 V	29
Figure 4.2	Iso-surfaces at 50 ⁰ C for i) 60, ii) 120, iii) 180, iv) 240, v) 300, vi) 360, vii) 420 and viii) 480 s with 22V	31
Figure 4.3	Iso-surfaces at (i) 37 ⁰ C, (ii) 38 ⁰ C, (iii) 39 ⁰ C, (iv) 41 ⁰ C, (v) 43 ⁰ C, (vi) 45 ⁰ C, (vii) 47 ⁰ C and (viii) 50 ⁰ C with 480 s and 22 V	33
Figure 4.4	Temperature versus time at the tip of one of the electrodes arm at 22 V	35
Figure 4.5	Temperature fields at 480 s at various electric voltages i) 25, ii) 30, iii) 35, iv) 40, v) 45, vi) 50 V.	36
Figure 4.6	Temperature versus time at the tip of one of the electrodes arm at i) 25, ii) 30, iii) 35, iv) 40, v) 45, and vi) 50 V.	38
Figure 4.7	Temperature versus time at the tip of one of the electrodes from 25 to 50 V	39

Figure 4.8 Comparison for temperature between Mellal *et al.* [9] (blue color) and present research (orange color). 40

CHAPTER 1

INTRODUCTION

1.1 Overview

Liver tumors (also known as hepatic tumors) are abnormal growths of liver cells on or above the liver. Different types of tumors in the liver can develop because the liver is made up of different cell types. This type of tumor is dangerous for the human body. Radiofrequency ablation is a committed minimally invasive treatment. Radiofrequency Ablation (RFA) treats Primary and secondary malignant tumors with minimal invasiveness, fewer side effects, and immunology stimulation compared to other treatment methods. The liver is a common site of metastatic tumors of different organs because of the large blood flow and filtering function of the liver. Surgery or transplantation is the preferred treatment for hepatic tumors, but up to 80% of liver cancer patients are not eligible for surgery because of poor baseline health and poor economic condition. However, most patients are not candidates for surgery due to different criteria such as multifocal disease, tumor size, location of the tumor in the main vessel, or coagulopathy. Thus, there is a demand for novel minimally invasive strategies for curing hepatic defects. Focal ablative therapies were developed and applied to treat hepatic malignancies. Unlike surgical treatment, objectionable therapies should not associate with complete sigmoidal or reduction of normal liver lobes. The most widely investigated relative relativity is cryoablation and radiofrequency (RF) release.

1.1.1 Malignant tumor

Liver cancer is a type of malignant tumor that starts in the liver and is the largest internal organ in the body. Most liver cancers develop from liver cells called hepatocytes. This cancer is referred to as primary liver cancer. Rarely, these can develop from cells lining the bile ducts or blood vessels. Other cancers spread to the liver from other areas, such as the colon, breast or lung. These are referred to as metastatic cancers.

Introduction

A malignant tumor is a term for a disease where abnormal cells divide uncontrollably and invade nearby tissues. Malignant cells can spread to other parts of the body through the blood and lymphatic system. If the cells continue to grow and spread, the disease can become life-threatening. There are many differences between healthy tissue and malignant tissue like as shown in figure 1.1. When enough cells are present, normal cells stop growing but cancer cells reproduce another cell. Normal cells have a normal shape but cancer cells always have an abnormal shape. Normal cells are either repaired or die (apoptosis is tolerated) when they are damaged or aged get cancer cells are either not repaired or apoptosis is not.

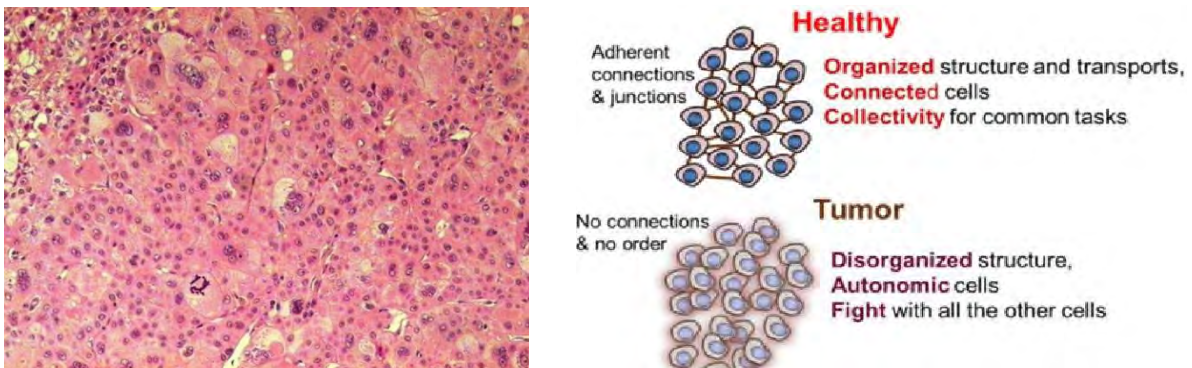


Figure 1.1: Differences between healthy and malignant tissue and malignant tumor in the liver

1.1.2 Radiofrequency ablation

Radiofrequency ablation (RFA) as a thermal ablative method is used to treat focal primary and secondary defect organs in the liver, lungs, kidneys, bones, and adrenal glands. It had shown that the clinical efficacy of RFE drops for tumor basics above 3 cm had discontinued sharply. The two advantages of radiofrequency current (more than previously used low-frequency AC or DC pulses) is that it does not directly stimulate nerve or heart muscle and can therefore be used frequently without the need for general anesthesia. It is desirable without very significant security loss in tissue treatment.

It removes the tumor from healthy tissue by heating the malignant tissue to the critical temperature that kills cancer cells. In this procedure, physicians would use a small electric

Introduction

probe to create a local heat source through which electric current runs. Radiofrequency ablation is used to remove tumors all over the world because it is safer than any surgery. How this procedure destroying the tumor from the liver is showed in figure 1.2.

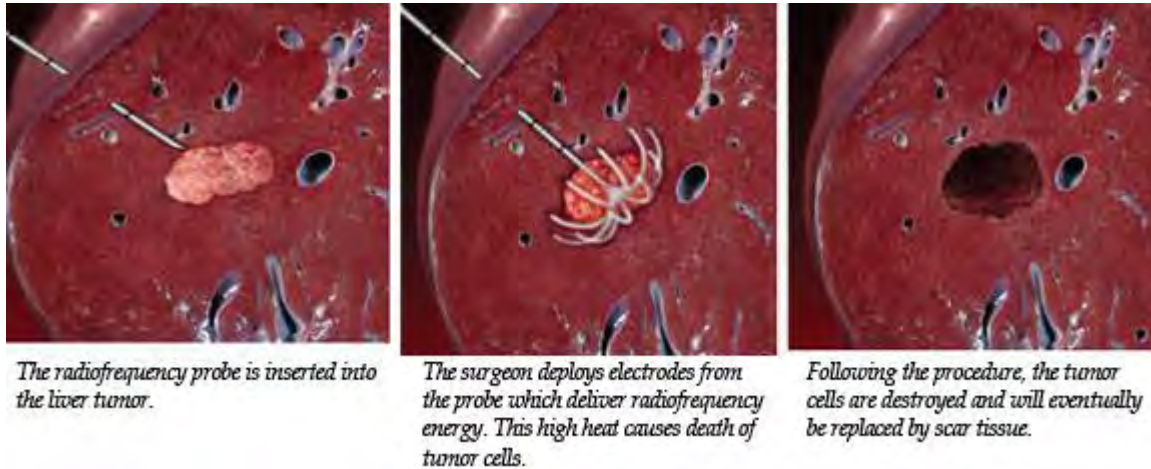


Figure 1.2: Radiofrequency ablation of liver

1.1.3 Radiofrequency probe

Radiofrequency (RF) probe is a thin needle that inserts through the skin and into the tumor. Tuberculosis of tuberculosis is examined by electrical current (radio-frequency energy) through the tumor or periodically through the tumor. It destroys tumor necrosis (cell death) and cancerous tissue. The dead cells eventually turn into a harmless strain.

The probe has three parts. They are trocar base trocar tip and four-electrode arms like as shown in figure 1.3. The trocar base is electrically insulated.



Figure 1.3: Radiofrequency probe with four electrode arms

1.1.4 Bioheat transfer equation

The Bioheat transfer equation is a parabolic partial differential equation. Grid points with individual variables have first formed to solve partial differential equations by the finite element method. In this study, the one-dimensional Bioheat transfer equation Flex-PDE has been solved using the finite material method.

Temperature-dependent tissue thermo-physical properties have been used and the Pennes's equation is solved by FEM analysis. The values of blood perfusion and heat production have been used in calculations for healthy tissue and tumor tissue.

The Bioheat equation governs heat transfer in the tissue

$$\rho C \frac{\partial T}{\partial t} + \nabla \cdot (-\kappa \nabla T) = \rho_b C_b \omega_b (T_b - T) + Q_{met} + Q_{ext}$$

Where ρ is the tissue density (kg/m^3), C is the tissue's specific heat ($\text{J}/(\text{kg}\cdot\text{K})$) and k is its thermal conductivity ($\text{W}/(\text{m}\cdot\text{K})$). On the right side of the equality, ρ_b gives the blood's density

Introduction

(kg/m^3), C_b is the blood's specific heat ($\text{J}/(\text{kg}\cdot\text{K})$), ω_b is its perfusion rate ($1/\text{s}$), T_b is the arterial blood temperature ($^\circ\text{C}$), while Q_{met} and Q_{ext} are the heat sources from metabolism and spatial heating, respectively (W/m^3).

1.1.5 Electric potential

Electrical potential is the amount of work required to transfer the electric charge (a column) to a certain point in an electric field to avoid radiation production with minimal or acceleration to avoid producing radiation at a certain point.

Tissue heating is a quadratic electrical used to describe the electric field and current density inspiring by radiofrequency energy. Under semi-static conditions the electrical potential can be solved using the Laplace equation:

$$\nabla \cdot [\sigma(T) \nabla V] = 0$$

1.1.6 Image-guided technique

Perfutenius image-guided technology [(CT), ultrasound, or magnetic resonance imaging] is used in the treatment of hepatic malignancy because it is minimally invasive than a surgery-related disease. When this procedure is performing, physicians always observe the probe position through this image-guided technique. CT- guided image is showed in figure 1.4.

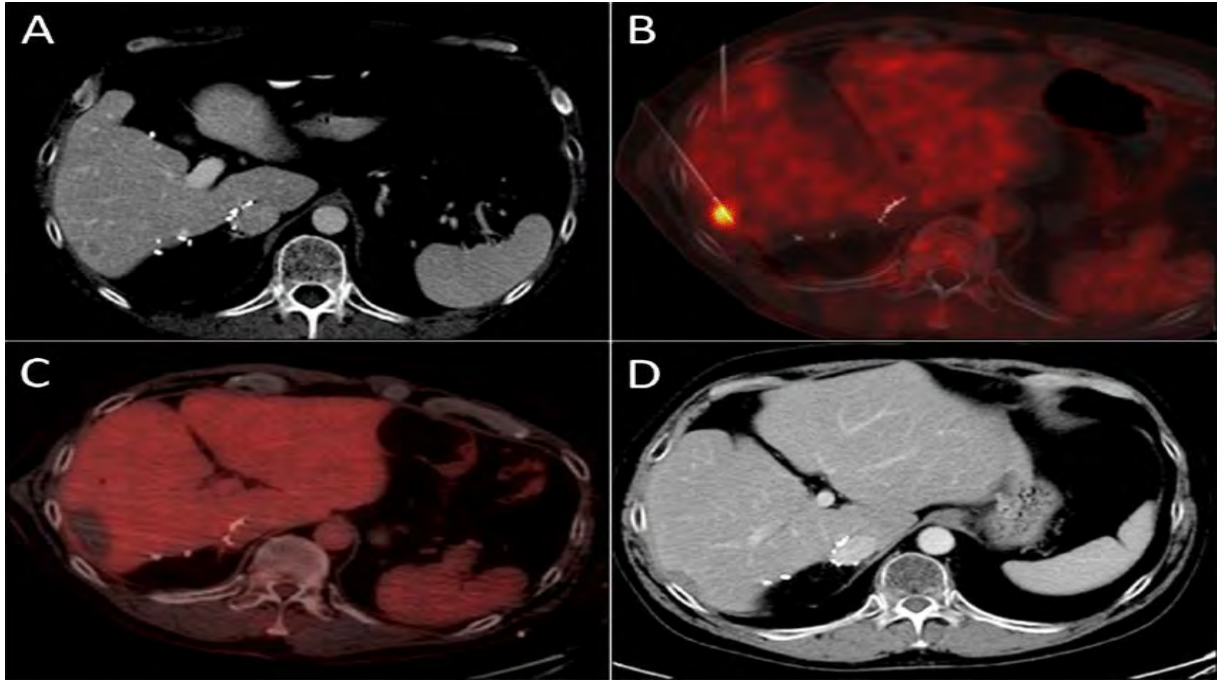


Figure 1.4: CT-guided radiofrequency ablation for liver treatment

1.2 Literature Review

Few researchers investigated hepatic tumor ablation by using analytical, experimental, and numerical methods. There are some important works presented below. Tungitkusolmun *et al.* [1] found highly non-uniform temperature distribution in the 2D model due to the presence of the bifurcated blood vessel. Fang *et al.* [2] designed a novel radiofrequency (RF) for large tumor ablation. Zhang *et al.* [3] investigated the relationship between the area of target tissue necrosis and the size of target tissue in pulsed RF ablation. Romero-Mendez *et al.* [4] presented an analytical solution for the RF ablation of tissue from a cooled cylindrical electrode. Hall *et al.* [5] performed a sensitivity analysis on a mathematical model of RF in the liver and showed the size of the 50°C isotherms was sensitive to the electrical properties of tissue while the heat source was active and to the thermal parameters during cooling. Suarez *et al.* [6] found the epicardial fat layer seriously impeded the passage of RF current, thus reducing the effectiveness of arterial wall RF ablation. Haemmerich *et al.* [7] observed that at 500 kHz there was little difference in RF current density and final tissue temperature between normal and cancer tissue. General principles and technique reviews each modality and modality selection were discussed by Knavel *et al.* [8].

Introduction

A 3D Finite Element Method (FEM) model for directional removing of a tumor is studied by Mellal *et al.* [9]. They presented that a directional probe with a curved cathode as a heating source can remove the malignant cells and protect the surrounding healthy cells. Rossmann *et al.* [10] demonstrated that tissue drug uptake directly correlates with heating duration for TSL based delivery. They also found that computational models were able to predict the spatial drug delivery profile, and may serve as a valuable tool in understanding and optimizing drug delivery systems. Sakree *et al.* [11] reported the first successful use of irreversible electroporation for the minimally invasive treatment of aggressive cutaneous tumors implanted in mice. They claimed that Irreversible electroporation is a new effective modality for non-thermal tumor ablation. A comparative investigation of heat sink effect in monopolar (MP) and bipolar (BP) radiofrequency ablation (RFA), and microwave (MW) ablation devices is conducted by Pillai *et al.* [12]. Adeyanju *et al.* [13] conducted that the distribution of electric field is highly dependent upon the electrode configuration, but the optimal configuration can be determined using numerical modeling. They claimed that their findings can help guide the clinical application of IRE as well as the selection of the best optimization algorithm to use is finding the optimal electrode configuration. Zhu *et al.* [14] studied that the mathematical model simulates the water evaporation and diffusion during radiofrequency ablation and may be used for the better clinical design of radiofrequency equipment and treatment protocol planning.

Sung *et al.* [15] suggested that the clinical results of the irreversible electroporation on liver tissue could be predicted through mathematical calculation. They investigated the static relationship between applied electric energy and the ablated area was mathematically and experimentally at 10 hours after applying irreversible electroporation. Berjano [16] analyzed the state-of-the-art in theoretical modeling as applied to the study of Radiofrequency ablation techniques. This study points out the present limitations, especially those related to the lack of accurate characterization of the biological tissues. Liu *et al.* [17] studied the characterization of the RF ablation-induced „oven effect“ with the importance of background tissue thermal conductivity on tissue heating. Their findings provided insight into the „oven effect“ (i.e. increased heating efficacy for tumors surrounded by cirrhotic liver or fat) and highlight the importance of both the tumor and the surrounding tissue characteristics when contemplating RF ablation efficacy. Ekstrand *et al.* [18] confirmed that preferential heating of the tumor

Introduction

during RFA exists in breast tissue in both the computer model and the in vitro study. They founded that the existing septa layers between the cancer tissue and the fatty tissue could have an additional electrical or thermal insulating effect, explaining the discrepancy between the in vitro study and the computer model. A model for the numerical simulation of radio frequency (RF) ablation of tumors with mono- or bipolar probes including the electrostatic equation and a variant of the well-known bio-heat transfer equation for the distribution of the electric potential and the induced heat is presented by Kroger *et al.* [19]. Gasselhuber *et al.* [20] demonstrated a synergistic effect between hyperthermia and chemotherapy, and clinical trials in image-guided drug delivery combine high-temperature thermal therapy (ablation) with chemotherapy agents released in the heating zone via low-temperature sensitive liposomes (LTSL). Trujillo and Berjano [21] studied that the different methods of modeling temperature dependence of electrical (σ) and thermal conductivities of biological tissue in radiofrequency ablation do not significantly affect the computed lesion diameter.

Payne *et al.* [22] developed a simulation tool kit that could be used both to optimize treatment protocols in advance and to train the less-experienced clinicians for RFA treatment of liver tumors. A modeling framework to evaluate macrophage interactions with the tumor microenvironment, enabling assessment of how these interactions may affect tumor progression is studied by Mahlbacher *et al.* [23]. Shafirstein and Feng [24] discussed the role of mathematical modeling in thermal medicine. Wang *et al.* [25] investigated that a tissue-mimicking breast gel phantom and its MR images were used to perform FEM 3D modeling and validation by experimental thermal ablation of the tumor. Similar patient-specific models can be created from preoperative images and used to perform finite element analysis to plan radiofrequency ablation. Haemmerich and Webster [26] presented results of a temperature-controlled 3-D FEM model of a RITA model 30 electrode. Nasrin *et al.* [27] studied blood flow analysis inside a stenotic artery using the Power-Law fluid model. Surita *et al.* [28] investigated a finite element analysis for optimizing antenna for microwave coagulation therapy.

From the above literature, it is observed that few kinds of research had been reported on hepatic tumor ablation. But necessary numerical studies are still required to monitor the uniform temperature distribution in the tissue around the electrode for hepatic tumor ablation.

In this research, tissue temperature distribution will be investigated numerically for hepatic ablation.

1.3 Motivation

In the light of the above discussions, it is seen that there have been a few works in the field of hepatic tumor ablation by Radiofrequency ablation. Unlike surgery, objectionable therapies are not associated with complete segmentation or loss of normal liver lobes. The most widely investigated relative relativity is cryoablation and radiofrequency (RF) release. Although the post-treatment recurrence rate of cryoablation was lower than that of RF, free surgery is generally necessary due to the large probe size and the risk of bleeding, in contrast, the RF elimination method is safe. There is a lot of research papers on radiofrequency ablation which used AC current but nobody uses DC current in their research. That's why there is some scope to work with this.

For this reason, necessary numerical studies are still required to monitor the uniform temperature distribution in the tissue around the electrode for hepatic tumor ablation, which forms the basis of the motivation behind selecting the present research.

1.4 Objectives

The specific objectives of the study are:

To simplify the traditional mathematical model [1] of RF heating with AC current for hepatic tumor ablation by approximating the energy with DC current. To solve the 3D, unsteady mathematical model using FEM. To monitor how the temperature increases with time in the tissue around the electrode. To find the optimum time needed for the critical temperature to heat the malignant tissue. To visualize the region where cancer cells die.

1.5 Possible Outcomes

Since the research proposal is applied to a large blood vessel of the liver which is useful in medical technology, several important outcomes from this research may be expected. These are summarized as follows:

According to this research, physicians will create a local heat source by inserting a small electric probe. This model will show us how the temperature increases with time in the tissue

around the electrode. This numerical procedure will remove the tumorous tissue by heating it above 318 to 323 K.

1.6 Outline of Thesis

A brief description of the present numerical investigation of radiofrequency hepatic tumor ablation in liver tissue using bio-heat transfer equation and electric currents have been presented in this thesis through five chapters as stated below:

Chapter 1 contains an introduction with the aim and objectives of the present work. This chapter also includes a literature review of the discussions, it is seen that there has been a good number of works in the field of hepatic tumor ablation by Radiofrequency ablation. The objectives of the present study have also been incorporated in this chapter.

The finite element method and Galerkin's weighted residual method are described in Chapter 2 which is used in the procedure. The description for the numerical simulation of bio-heat transfer has been included. In addition, the advantage of numerical analysis, meshing, accuracy, and grid sensitivity test has been illustrated in this chapter.

In Chapter 3, hepatic tumor RF ablation by using Bioheat equation and electric current has been described in this chapter. The electrical and thermal properties, governing equation, solution procedure are also discussed properly in this chapter.

The result and discussions are described properly in chapter 4. The effects of time and electric voltage have been discussed in this chapter. Temperature distribution, Iso-surfaces, and point graphs have been shown at different times, temperatures, and electric voltage in this chapter.

Chapter 5 concludes remarks of the whole research and the recommendations for future research.

Finally, all references are included.

CHAPTER 2

NUMERICAL TECHNIQUES

2.1 Introduction

Computational Fluid dynamics is the given term for presenting and solving the fluid flow and related equations in a computer. The power of modern workstations and the relatively low cost, high quality of commercial CFD codes now available together, a very attractive tool for designers and engineers in the CFD process industries, and an effective vehicle and mass transfer field for many research workers in the heat. Although CFD is about solving complex equations, the real challenges revolve around understanding physics and how the necessary elements of the problem can be present in terms of equations and boundary conditions. The nonlinearity and physics complexity present in inflow equations are such that CFD cannot potentially replace all physical experiments in the future. However, CFD can help to reduce the quantity of costly experimental work and help design better experiments to increase our understanding and predictive skills.

CFD has applied to a wide range of research and engineering problems in many fields of study and industry, including aerodynamics and aerospace analysis, weather simulation, natural science and environmental engineering, industrial system design and analysis, biological engineering, fluid flow, and heat transfer, and engine and combustion analysis.

Mathematical modeling and Numerical analysis are two essential components of CFD. Sometimes it is difficult to separate them. Mathematical modeling is about expressing the problem in a mathematical form with reasonably accurate differential equations and adequate boundary conditions. Although it is seen directly, it is the most difficult and demanding task that most engineers face when using CFD. You have to decide how detailed the CFD calculation is going to be and how detailed it needs to be to present the significant processes involved in a problem. The second component of CFD relates to the presentation of the above equations in computers and the numerical aspects of solving them. The first task is to choose an integrated system and mesh that will be able to give adequate solutions to the geometry and physics of the problem. The second task is to digitize the differential equations in the form of

Numerical techniques

their differences, in a way that results in an accurate and stable set of algebraic equations suitable for numerical manipulation. The ultimate numerical task is to use a solution process that will solve discrete equations quickly and 'accurately' without making unnecessary claims about hardware (memory, disk space, and central processor speed).

2.2 Advantage of numerical analysis

Fluid flow, heat, and mass transfer problems can analyze theoretically or experimentally. From an economic point of view, the experimental investigation of these problems did not attract much attention due to their insufficient flexibility and applications. However, often experimental investigations are necessary to validate the numerical method. Any change in geometry requires a separate experimental system/setup and the boundary conditions of the systems for their investigation. The involvement of time is also a reason to make it appealing. Theoretical analyzes can perform through analytical methods or numerical methods. Analytical solution methods for solving practical problems are not very popular. Numerical methods are powerful problem-solving tools capable of handling large systems of equations, complex geometry, etc., which are often impossible to solve analytically. Generally, closed-form solutions are very ideal cases and the results obtained for specific problems can usually be found with identical boundary conditions. Numerical methods are an easy way to find solutions of problems for practical interest because it reduces superior mathematics to basic arithmetic operations.

2.3 The steps of a numerical solution

The steps from various components of the numerical solution are as follows:

2.3.1 Mathematical model

The starting point of any numerical method is the development of a mathematical model consisting of a partial differential equation or a set of integral differential equations and boundary conditions. A solution method has been designed for a specific equation. A general-purpose solution, such as one that applies to all flows, is unreasonable, although not impossible, and with most general-purpose tools, they are usually not optimal for a single application.

2.3.2 Discretization techniques

After selecting the mathematical model, a suitable rational method must be selected, i.e. a method of equating differential equations by a system of algebraic equations for variables in some set of isolated positions of space and time. There are several approaches, the most important of which are: finite difference (FD), finite volume (FV), and finite element (FE) methods.

2.3.3 Meshing

The isolated locations where the variables need to be calculated are defined by a mesh that covers the geometric domain where the problem needs to be solved. It divides the solution domain into a finite number of sub-domains called finite elements, amount of control, etc.

2.3.4 Accuracy

Numerical solutions to physical events are only approximate solutions. Numerical solutions typically involve three types of systemic errors.

- Modeling errors that occur due to differences between actual physical phenomena and the correct solution of the mathematical model.
- Wisdom errors are defined as the difference between the correct solution of the equation of the model and the correct solution of that algebraic method of the equation obtained by considering these equations
- Defined as the difference between iteration errors, repetition of algebraic systems of equations, and correct solutions.

It is important to identify these flaws and distinguish them. Different errors can negate each other so that sometimes the solution obtained from a thick mesh pretends to be better compliant with the test than the solution of a fine mesh, which should be more accurate. Therefore, the counterfeit must be handled very carefully.

2.3.5 Grid system

Before running the CFD simulation we need to determine the size of the effective grid. The size of the effective grid means it is small enough to reduce errors from wastage due to the

Numerical techniques

grid and large enough to save the computing source. To get a reliable simulation result, the grid conversion study should be done before looking deeper into the deep stream. No solution should be adopted if the grid is not distinct. This means that a computer runs repeatedly with fine and fine grids until the results change at any point in space.

2.3.6 Solution technique

Practical applications of the finite element method simultaneously lead to large systems of linear algebraic equations. Fortunately, finite component equation systems have some features that allow them to reduce storage and computing time. Restricted material equation systems: symmetrical, positively precise, and rare. Synthesis allows storing half of the matrix with diagonal entries. Positive specific metrics are characterized by large positive entries in the main triangle. The solution can be run without pivoting. A rare matrix has more entries than non-zero entries. Sparsity can be used to economize storage and calculations. Solution methods for linear equation systems can be divided into two major groups: direct methods and iteration methods. Direct solution methods are used for medium-sized problems. Repeat methods for larger problems require less computing time and are more desirable than that. The choice of solver depends on the type of grid and the number of nodes involved in each algebraic equation.

2.4 Finite Element Method

The Finite Element Method (FEM) is a widely used method for solving the number of differential equations arising in engineering and mathematical modeling. Areas of common problem interest include structural analysis, heat transfer, fluid flow, mass transport, and traditional theoretical fields of electromagnetic potential. FEM is a fixed numerical method for solving partial differential equations between two or three space variables (i.e. some boundary value problems). To solve a problem, FEM divides a large system into smaller, simpler parts called finite components. This is achieved by considering a specific space in the dimensions of space, which is applied by constructing a lattice of objects: the numerical domain for a solution, which has a finite number of has a boundary value problem. The introduction of a finite element method is finally the result of a system of algebraic equations. The method approximates the unknown function above the domain and the simple equations that model these finite elements are then combined into a larger system of equations that models the

Numerical techniques

whole problem. It then uses a variety of methods from conversion calculus to approximate solutions by reducing FEM-related error functions.

Working out of the method involves dividing the problem domain into a set of subdomains, representing each subdomain with a set of basic equations with the main problem, and systematically rearranging all sets of elemental equations for a global system of equations for final calculations. Solution strategies are known in the global method of equations and can be calculated from the initial values of the main problem to get the answer to a number. In the first step above, material equations are general equations that infer the original complex equations to be studied locally, where the original equations are often partial differential equations (PDEs). To approximate the explanation of this process, the phenytoin material is usually introduced as a special case of Galerkin's method. The process is, in mathematical terms, an integral structure of the internal product of the remaining and weighted activities and set in the integral void. In general, it is a process that reduces proximity error by fitting the trial function in PDE. Residues Errors caused by trial functions and weight functions are multilevel approximation functions that project residues. The process removes all spatial derivatives from the PDE, thus approximately locally with the PDE

- A set of algebraic equations for fixed state problems.
- A set of general differential equations for a transient problem

These equation sets are element equations. The underlying PDEs are linear and vice versa. Integral equation sets that arise in fixed-state problems are solved using numerical linear algebraic methods, while general differential equation sets that arise in transient problems are solved by numerical integration using standard techniques such as Euler's method or Range-Katta's method. In the above step (2), global equations are created from material equations by converting coordinates from local nodes of subdomains to global nodes of domains. This spatial transformation involves appropriate orientation adjustments as related to the reference coordinate system. The process is often driven by FEM software using integrated data generated from sub-domains. FEM is best understood from the practical application of what is known as finite element analysis (FEA). It is a valuable tool for analyzing engineering as it is applied in engineering. This includes the use of fake generation technology to break down complex problems into smaller components, as well as the use of software programs coded

Numerical techniques

with FEM algorithms. The complex problem in the application of FEA is usually an underlying physics such as an Aller-Bernoulli beam equation, heat equation, or Navier-Stokes equations expressed in PDE or integral equations, but the fragmented smaller components represent different areas of the complex problem physiological system.

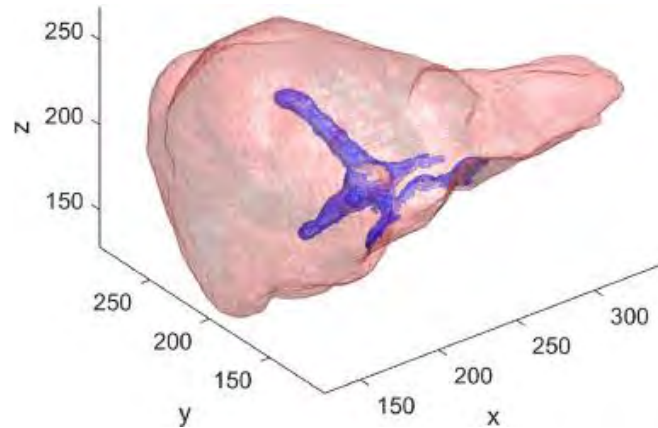


Figure 2.1: Finite element simulation of liver

2.5 Galerkin's Weighted Residual Technique

The Weighted Residue Method (WRM) is an approximate technique that approximates the solution of differential equations by the linear combination of trials or shape functions with unknown coefficients. The approximate solution is replaced by a differential equation conducted as a result of an error or residual. Until the end, the remnants of the WRM have to disappear at the mean points or be made as small as possible, depending on the weight efficiency to find unknown coefficients. The weighted residual method can be solved by various methods. Some of the standard methods are the point collocation method, subdomain collocation method, least square method, and Galerkin's method.

In Galerkin's version of the weighted residue, the weight functions are selected as their own trial function. We usually use this method to develop limiting material equations for the field Problems. So, in Galerkin's method, we can set

$$W_i = N_i, (i = 1, 2, \dots, n).$$

Numerical techniques

Galerkin's method produces a symmetric positive definite coefficient matrix if the differential operator is self-adjoint. Galerkin's method requires less computational effort compared to the least square method.

Suppose we have a linear differential operator D acting on a function u to produce a function p .

$$D(u(x)) = p(x).$$

We wish to approximate u by a function \tilde{u} which is a linear combination of basis functions chosen from a linearly independent set. That is,

$$u \cong \tilde{u} = \sum a_i \Phi_i, \text{ where } i = 1, \dots, n$$

Now, when substituted into the differential operator D , the result of the operations is not, in general, $p(x)$. Hence an error or residual will exist:

$$E(x) = R(x) = D(\tilde{u}(x)) - p(x) \neq 0.$$

The notion in the MWR is to force the residual to zero in some average sense over the domain. That is

$$\int_x R(x) W_i dx = 0; \text{ where } i = 1, \dots, N$$

Here the number of weight functions W_i is exactly equal to the number of unknown constants a_i in \tilde{u} . The result is a set of n algebraic equations for the unknown constants a_i . The derivative of the residual concerning the unknown a_i , the derivative of the approximating function is used. That is, if the function is approximated as in 2.1, then the weight functions are

$$W_i = \partial \tilde{u} / \partial a_i$$

These are then identical to the original basis functions appearing in 2.1

$$W_i = \partial \tilde{u} / \partial a_i = \phi_i(x)$$

CHAPTER 3

NUMERICAL MODELING OF RADIOFREQUENCY HEPATIC TUMOR ABLATION

3.1 Introduction

There has been a little numerical study of hepatic ablation. One method for removing cancerous tumors from healthy tissue is to heat the malignant tissue to a critical temperature that kills the cancer cells. Tungitkusolmun *et al.* [1] simulated a Three-dimensional finite element method model for hepatic ablation by using AC currents. I have made some simplifications to approximate the energy with DC currents. I have established realistic FEM to better understand how the models of RF ablation model are presently flowing around the liver tissue near them. The purpose of the heating process is to kill malignant cells with less collateral damage to nearby healthy tissues. The configuration of the initial probe that we modeled, a RITA Medical Systems Model 30, which is the most commonly, utilized clinical system [1]. Direct RF is investigated regularly in the tumor of the liver under CT or ultrasound once the guidance is in place, surgeons place a four-tine star an umbrella-like array, and RF current. The following technique accomplishes the localized heating by inserting a four-armed electric probe through which an electric current runs. Equations for the electric field for this case appear in the Electric Currents interface, and this example couples them to the bioheat equation, which models the temperature field in the tissue. The heat source resulting from the electric field is also known as resistive heating or Joule heating. This medical procedure removes the tumorous tissue by heating it above 45 °C to 50 °C. Doing so requires a local heat source, which physicians create by inserting a small electric probe.

3.2 Physical Model

This research has accomplished the localized heating by inserting a four-armed electric probe through which an electric current runs. The probe is made of a trocar (the main rod). The trocar tip and trocar base are of radius 0.91 mm and distances from the plane are 10 and 50 mm respectively. The electrode arm has a radius of 0.27 mm. The trocar is electrically insulated except near the electrode arms. An electric current through the probe creates an

Numerical modeling of radiofrequency tumor ablation

electric field in the tissue. The field is the strongest near the probe and generates resistive heating, which will dominate around the probe's electrode arms because of the strong electric field. The model has approximated the body tissue with a large cylinder of height and radius of 120 mm and 50 mm respectively. The tumor is located near the center of the cylinder with the same thermal properties as the surrounding tissue. The model has located the probe along the cylinder's centerline such that its electrodes span the region where the tumor is located. The geometry also includes a large blood vessel whose radius is 5 mm and 120 mm distance from the plane. The model geometry is shown in figure 3.1 where a four-armed electric probe is in the middle, which is located next to a large blood vessel.

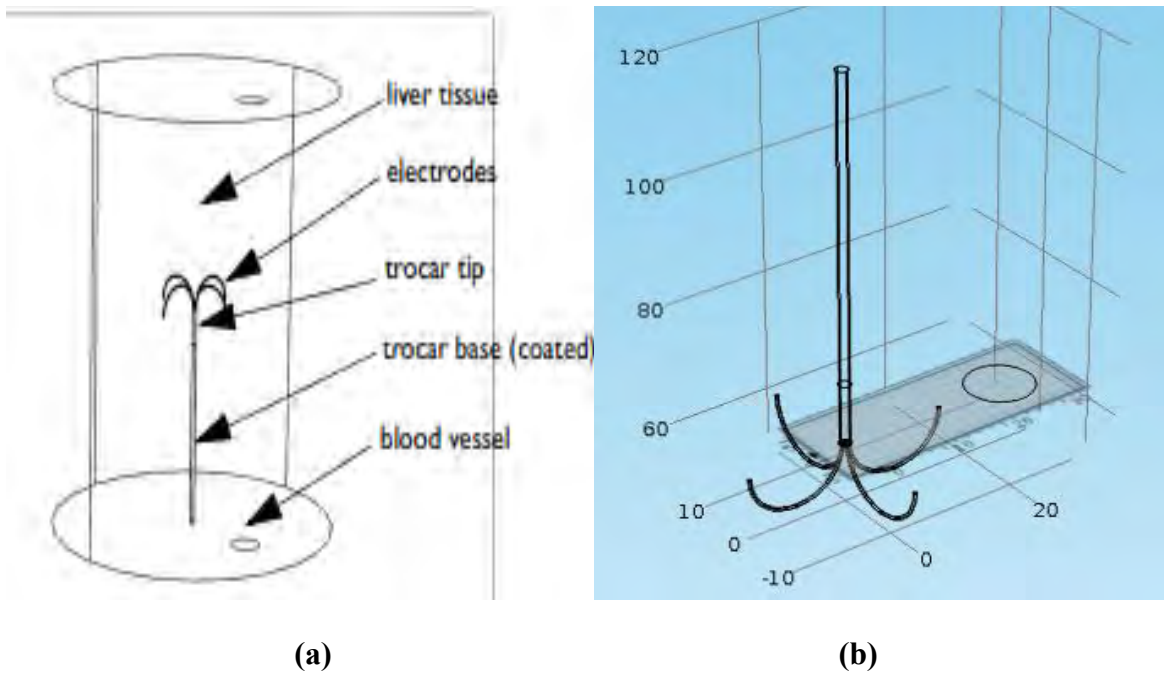


Figure 3.1: (a) Cylindrical domain with the four-armed electric probe and (b) computational domain

The whole architecture is reported in figure 3.2(a-b). The one we have displayed the liver tissue in the cylindrical form in 3D view and another in zoom view. Probes have been applied to remove suspected tumors.

Numerical modeling of radiofrequency tumor ablation

3.3 Governing equations

This model uses the Bioheat transfer interface and the Electric Currents interface to implement a transient analysis. Equations for the electric field for this case will appear in Electric Currents with a coupling of Bioheat transfer interface.

This model uses the Celsius temperature scale, which is more convenient for models involving the Bioheat equation. The model approximates the body tissue with a large cylinder and assumes that its boundary temperature remains at 37°C during the entire procedure. The tumor is located near the center of the cylinder and has the same thermal properties as the surrounding tissue. The model locates the probe along the cylinder's centerline such that its electrodes span the region where the tumor is located. The geometry also includes a large blood vessel.

The Bioheat equation will govern heat transfer in the tissue and various parts of the probe. A temperature of 310.15 K will be assumed at the outer boundaries of the cylinder and the walls of the blood vessel. Heat flux continuity will be maintained on all other boundaries. At the electrode and cylinder's outer boundaries the potential will be 22 and 0 V, respectively.

The governing Bioheat equation for the liver tissue and probe (not blood vessel) is as follows:

$$\rho C \frac{\partial T}{\partial t} + \nabla \cdot (-\kappa \nabla T) = \rho_b C_b \omega_b (T_b - T) + Q_{met} + Q_{ext} \quad (3.1)$$

Where ρ is the tissue density (kgm^{-3}); C is the tissue's specific heat ($\text{Jkg}^{-1}\text{K}^{-1}$), and κ is its thermal conductivity ($\text{Wm}^{-1}\text{K}^{-1}$). On the right side of the equality, ρ_b gives the blood's density (kgm^{-3}); C_b is the blood's specific heat ($\text{Jkg}^{-1}\text{K}^{-1}$); ω_b is its perfusion rate (s^{-1}); T_b is the arterial blood temperature ($^{\circ}\text{C}$); while Q_{met} and Q_{ext} are the heat sources from metabolism and spatial heating, respectively (Wm^{-3}).

In this study, Q_{met} is neglected since it is small. The external heat source results from the heat generated by the electric current field:

$$Q_{ext} = \mathbf{J} \cdot \mathbf{E} \quad (3.2)$$

Where \mathbf{J} is the current density (Am^{-2}) and \mathbf{E} is the electric field intensity (Vm^{-1}).

Thus equation (3.1) becomes for liver tissue

$$\rho C \frac{\partial T}{\partial t} + \nabla \cdot (-\kappa \nabla T) = \rho_b C_b \omega_b (T_b - T) + \mathbf{J} \cdot \mathbf{E} \quad (3.3)$$

In this model, the bio-heat equation also models heat transfer in various parts of the probe with the appropriate values for the specific heat, C ($\text{Jkg}^{-1}\text{K}^{-1}$), and heat conductivity, κ ($\text{Wm}^{-1}\text{K}^{-1}$). For these parts, all terms on the right are zero i.e.

$$\rho C \frac{\partial T}{\partial t} + \nabla \cdot (-\kappa \nabla T) = 0 \quad (3.4)$$

The governing electric current conservation equation for the liver tissue, blood vessel, and the probe is as follows:

$$-\nabla \cdot \mathbf{J} = \mathbf{Q}_j \quad (3.5)$$

Where $\mathbf{J} = \sigma \mathbf{E} - \mathbf{J}^e$ and $\mathbf{E} = \nabla V$

Thus equation (3.5) becomes

$$-\nabla \cdot (\sigma \nabla V - \mathbf{J}^e) = \mathbf{Q}_j \quad (3.6)$$

Where V is the potential (V), σ the electrical conductivity (Sm^{-1}), \mathbf{J}^e an externally generated current density (Am^{-2}), \mathbf{Q}_j the current source (Am^{-3}). Here both \mathbf{J}^e and \mathbf{Q}_j are zero.

The governing equation, therefore, simplifies into

$$-\nabla \cdot (\sigma \nabla V) = 0 \quad (3.7)$$

The boundary conditions for the Bioheat equation are:

$T = T_b$ on the exterior boundaries of the liver tissue

$\mathbf{n} \cdot (\kappa \nabla T) = 0$ on all interior boundaries (heat flow continuity condition)

$T_0 = 310.15 \text{ K}$ initial temperature in all domains.

The boundary conditions for the electric currents interface are:

$V = 0$ on the exterior boundaries of the liver tissue, blood vessel, and trocar base

$V = V_0$ on the boundaries of the electrode and trocar tip

$\mathbf{n} \cdot \mathbf{J} = 0$ on all other boundaries (electric current flow continuity condition)

3.4 Thermal properties

The thermo physical properties of the blood, Temperature, and Electric potential are taken from [1-9] and given in Table 3.1. Thermal and electrical properties of the 3D model inspired by literature have been included in Table 3.2. Let, the properties of liver tissue do not vary with temperature.

Table 3.1: Values of basic blood properties

Name	Expression	Description
ρ_b	1000 [kgm^{-3}]	Density, Blood
C_b	4180 [$\text{Jkg}^{-1}\text{K}^{-1}$]	Heat capacity, blood
ω_b	6.4e-3 [s^{-1}]	Blood perfusion rate
T_b	37 [$^{\circ}\text{C}$]	Arterial blood temperature
T_0	310.15 [K]	Initial domain temperature
V_0	22 [V]	Electric voltage

Table 3.2: Thermal and electric properties

Name	Unit	Liver	Blood	Electrode	Trocar tip	Trocar base
Electric conductivity, σ	Sm^{-1}	0.333	0.667	1e8	4e6	1e-5
Thermal conductivity, κ	$\text{Wm}^{-1}\text{K}^{-1}$	0.512	0.543	18	71	0.026
Density, ρ	Kgm^{-3}	1060	1000	6450	21500	70
Heat capacity at constant pressure, C_p	$\text{Jkg}^{-1}\text{K}^{-1}$	3600	4180	840	132	1045

3.4 Solution procedure

By Using Galerkin's weighted residual technique of finite element method the solution domain has been discretized into meshing which consists of four types of a finite number of elements such as triangular, quadrilateral, edge, and vertex. The unknown variables of temperature and electric potential have been expanded at each nodal degree of freedom and

solved. The relative error for each variable between consecutive iterations has been recorded below 0.0001. To obtain the temperature field (as a function of time), the unsteady solution has been obtained at a time range of 0 to 1000 s. This numerical model has shown how the temperature increases with time in the tissue around the electrode. After every 60 s, temperature distribution has been observed and noted required time to reach a temperature at least 323 K where cancer cells will die. In this method, the solution domain has been discretized into finite element meshes, which have been composed of non-uniform tetrahedral and triangular elements inside the domains and boundaries, respectively. Then the nonlinear governing partial differential equations have been transferred into a system of integral equations by applying Galerkin's weighted residual method. The basic unknowns for the governing partial differential equations are the velocity components Temperature T and the Electric Potential V . The six nodes with triangular elements have been used in this numerical research. The nonlinear algebraic equations so obtained have been modified by the imposition of boundary conditions. These modified nonlinear equations have been transferred into linear algebraic equations by using Newton's method. Finally, these linear equations have been solved by using the triangular factorization method. The convergence criterion for the solution procedure has been defined as $|\Psi^{n+1} - \Psi^n| < \varepsilon$, where n is the number of iteration and is a function of T and V .

3.4.1 Mesh generation

Meshing the complicated geometry makes the finite element method a powerful technique to solve boundary value problems occurring in a range of engineering applications. Figure 3.4 depicts the mesh configuration of the present physical domain with non-uniform tetrahedral and triangular elements triangular finite elements. In the fine type of meshing the computational region consists of four types of elements as tetrahedral, triangular, edge, vertex, and the number of elements is 72052, 5290, 976, 76, respectively. Thus, the total element size is 78394. In this fine type of meshing, minimum and average element size 0.002334 m and 0.7004 m respectively, element volume ratio is 9.668E-6, mesh volume is 938700.0 mm³. The resolution of narrow regions is 0, and the maximum element growth rate is 5.35. The element quality histogram has been shown in figure 3.5.

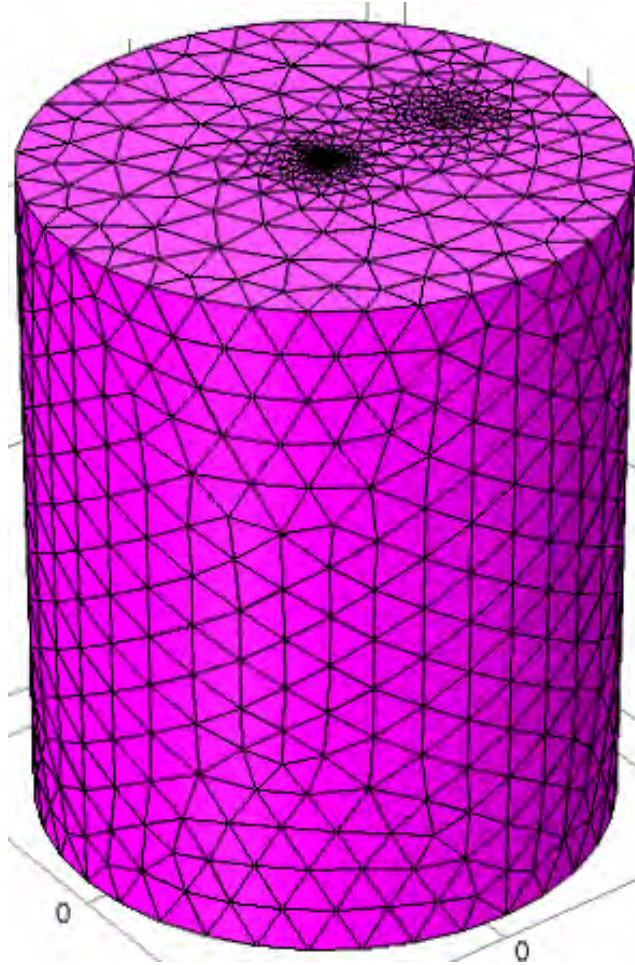


Figure 3.4: Finite element meshing of 3D domain

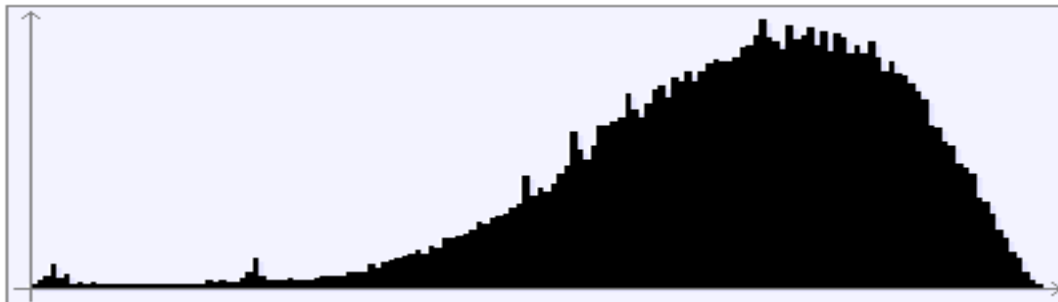


Figure 3.5: Element quality histogram

3.4.2 Code validation

To authenticate the exactness of the present numerical technique, the obtained results in the special case have been validated with the results obtained by Surita *et al.* [28] to authenticate

the accuracy of the present numerical methodology. This validation has been shown in Figure 3.6. They investigated finite element analysis for optimizing antenna for microwave coagulation therapy. The code validation has been conducted while employing the parameters $P = 10 \text{ W}$ and $f = 2.45 \text{ GHz}$ and the surface temperature distribution of the liver tissue has been shown in this figure. A very good agreement is found between the present code result and that of Surita *et al.* [28]. This flattering comparison provides confidence in the numerical results to be reported subsequently.

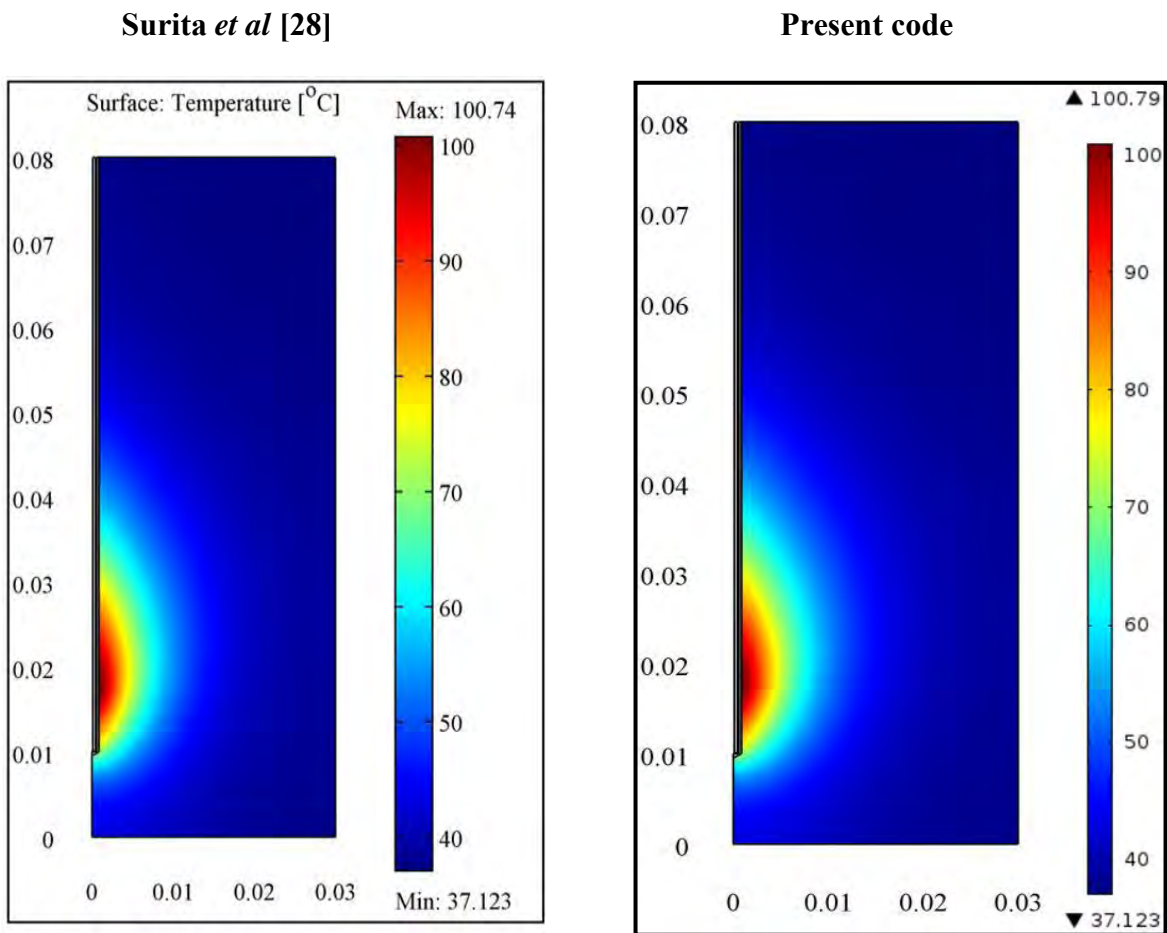


Figure 3.6: Code validation of the surface temperature distribution in liver tissue between Surita *et al.* [28] and present code

CHAPTER 4

RESULTS AND DISCUSSIONS

4.1 Introduction

The liver is a common site of metastatic tumors from different organs because of the large blood flow and filtering function of the liver. Surgery or transplantation is the preferred treatment for hepatic tumors, but up to 80% of liver cancer patients are not eligible for surgery because of poor baseline health and poor economic condition. A 3D liver tumor removal model has been simulated using COMSOL Multiphysics and results have been reported in the following section. The bioheat equation and electric current interface have been solved numerically using FEM. The Joule effect has been used to heat the target tissue using a cathode as a guide Heater necrotic tissue and temperature have been recorded. The results have been shown in terms of temperature fields, the plot of iso-surfaces for different times as well as temperatures and temperature versus time at the tip of the electrode for the effects of time and electric voltage. In this research, tissue temperature distribution has been investigated numerically for hepatic ablation. Also, the visualization of the region where cancer cell dies has been shown in this numerical procedure.

4.2 Effect of Time

Figure 4.1 (i-viii) shows the surface temperature distribution for various times like 60, 120, 180, 240, 300, 360, 420, and 480 s at fixed 22 V. Its features the wound formed in this case was also like a mushroom, which was slightly outstanding due to the cooling effect on the blood vessels. All figure of figure 4.1 shows the temperature distribution after 60 s heating. It made clear to us that the temperature distribution is gradually increasing every 60 seconds. The temperature is increasing around the electrode located at the center of the tumor. There is a big difference in temperature at a time from 60 to 300 s. But a little significant change has been shown in temperature from 360 to 480s.

Results and discussions

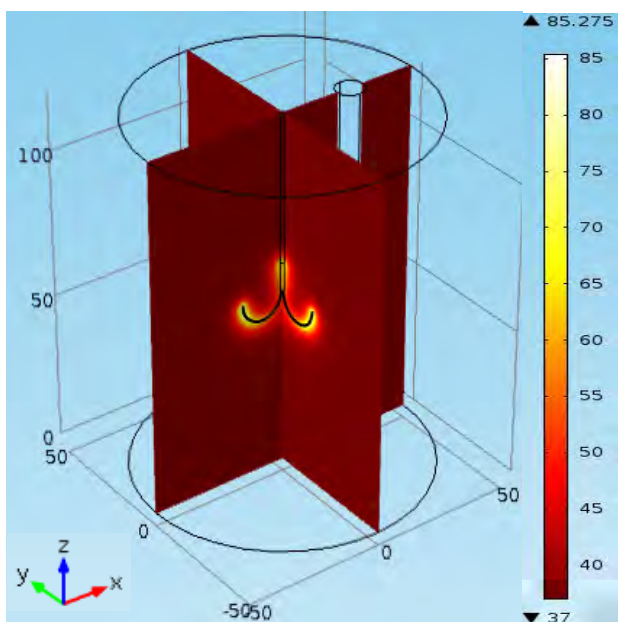
Figure 4.2 (i-viii) shows the Iso-surfaces at 50°C for various times like 60, 120, 180, 240, 300, 360, 420, and 480 s at fixed 22 V. The damage of the malignant tumor tissue is quite low after 1-minute heating.

Due to the increase in ablation time, the tumor tissue has been damaged greatly. When the temperature has reached 50°C at various times, then the region can visualize where cancer cells die. It has been shown that cancer cell dies approximately after 8 minutes in figure 4.2 (viii).

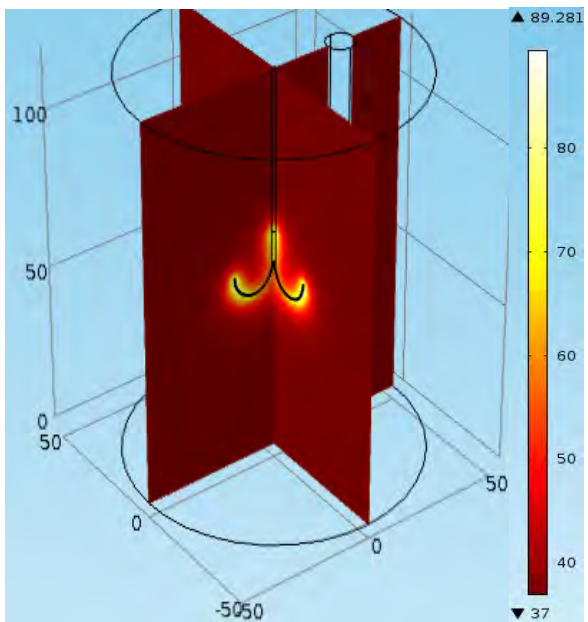
Figure 4.3 (i-viii) shows the Iso-surfaces at various temperatures like 37°C , 38°C , 39°C , 41°C , 43°C , 45°C , 47°C , and 50°C at 480 s with fixed 22 V. The size of the malignant tumor tissue is quite low at 37°C after 480 s. Due to the increase in temperature through the electrode in tissue, the tumor size has been reduced greatly.

Figure 4.4 shows the temperature distribution versus various time ranges from 0 to 1000 s at a fixed 22 V at the tip of one of the electrodes. The temperature rises quickly until it reaches a steady-state temperature of about 90°C . After that, there is no significant change in temperature.

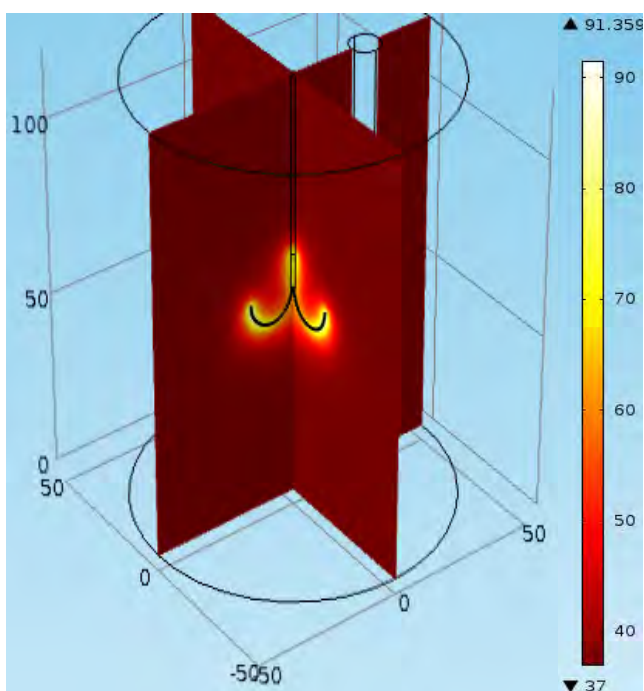
Results and discussions



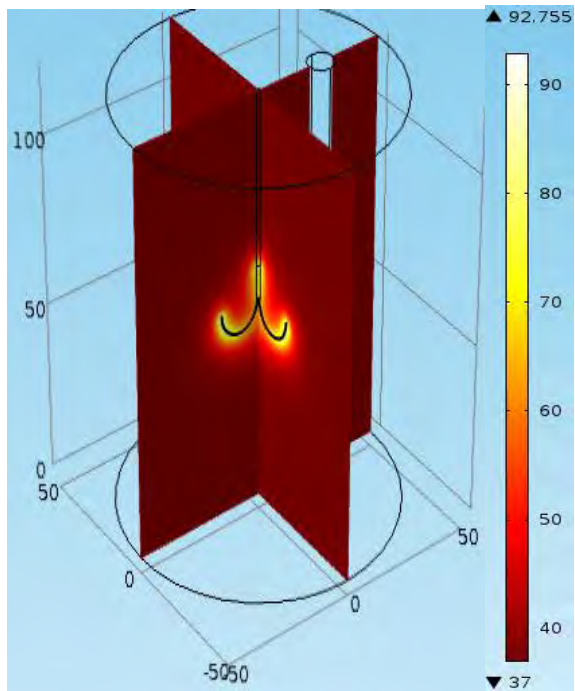
(i)



(ii)



(iii)



(iv)

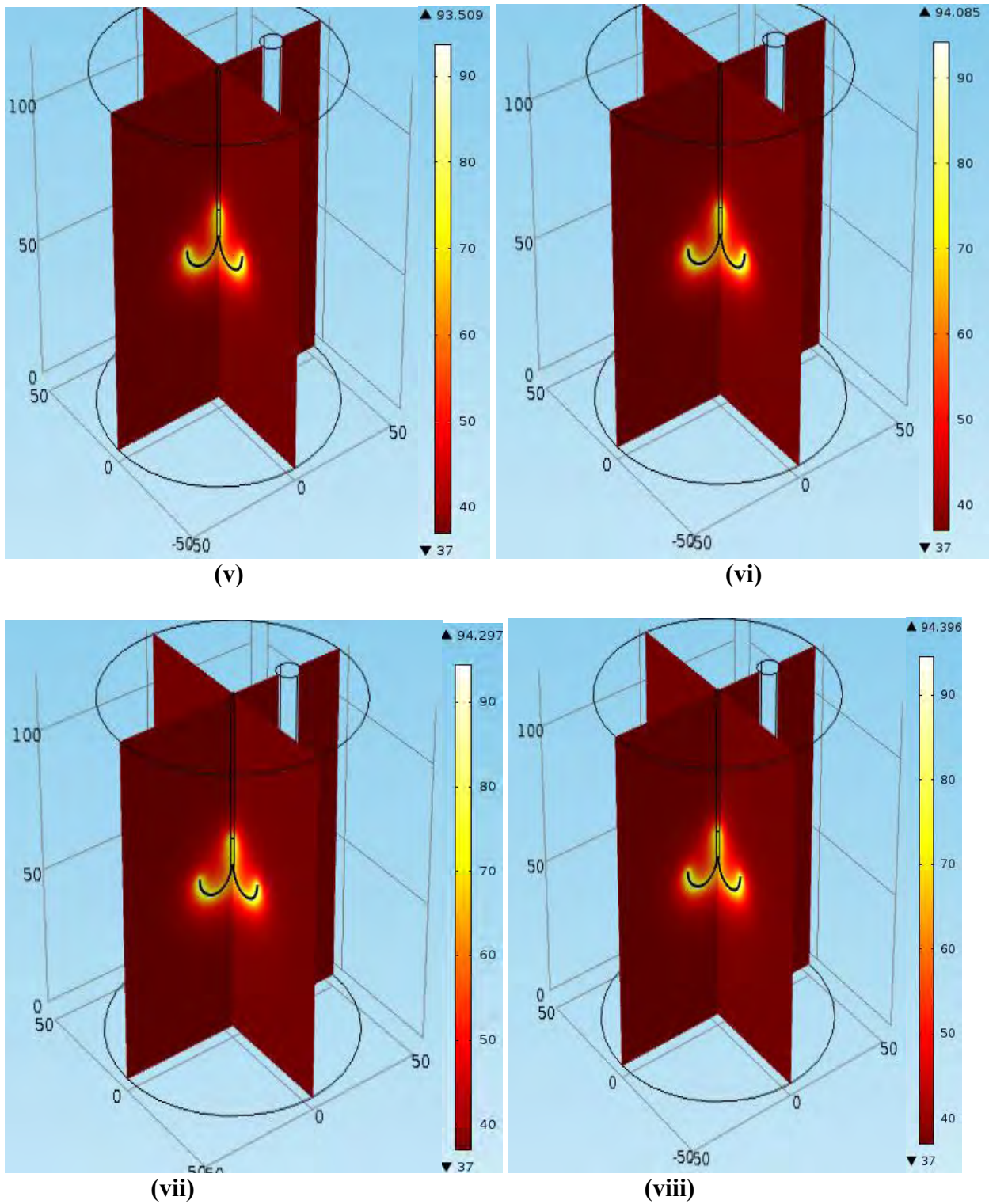
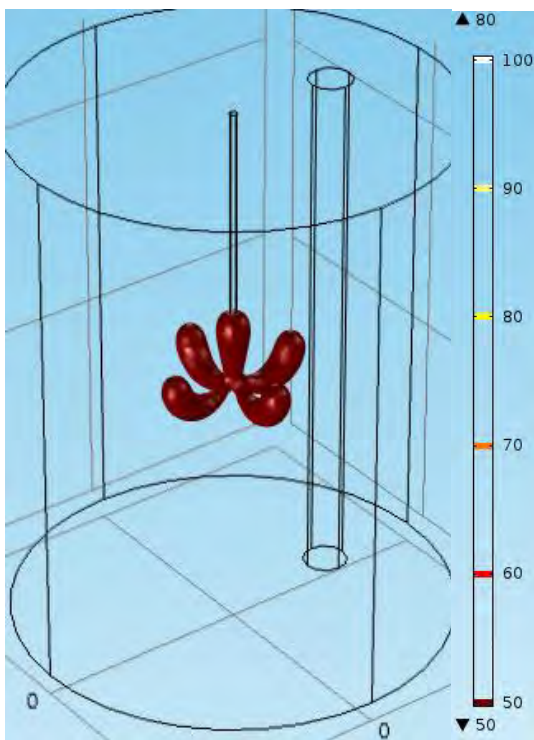
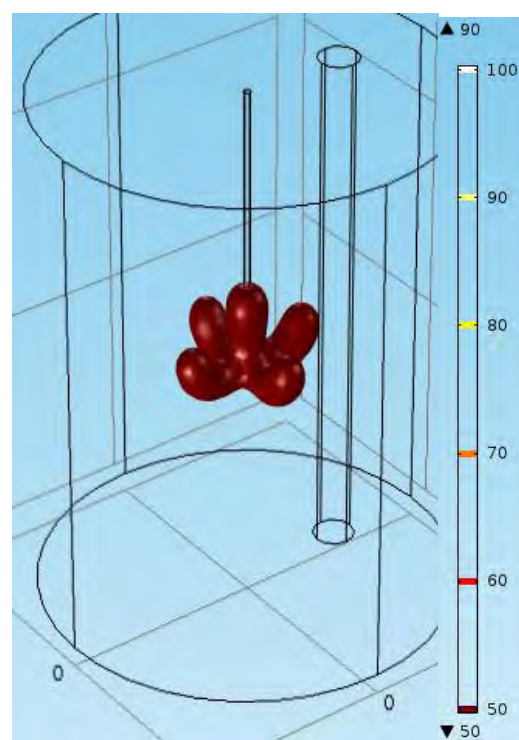


Figure 4.1: Temperature fields for various time (i) 60, (ii) 120, (iii) 180, (iv) 360, (v) 420 and (vi) 480 s at 22 V

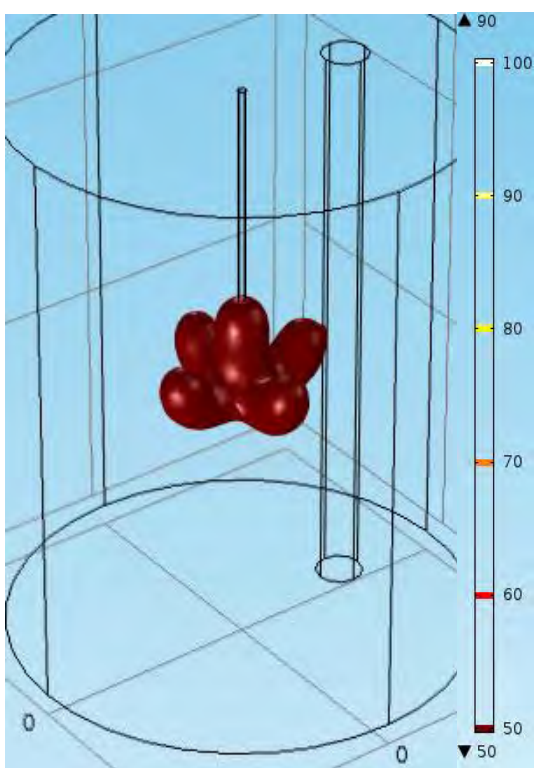
Results and discussions



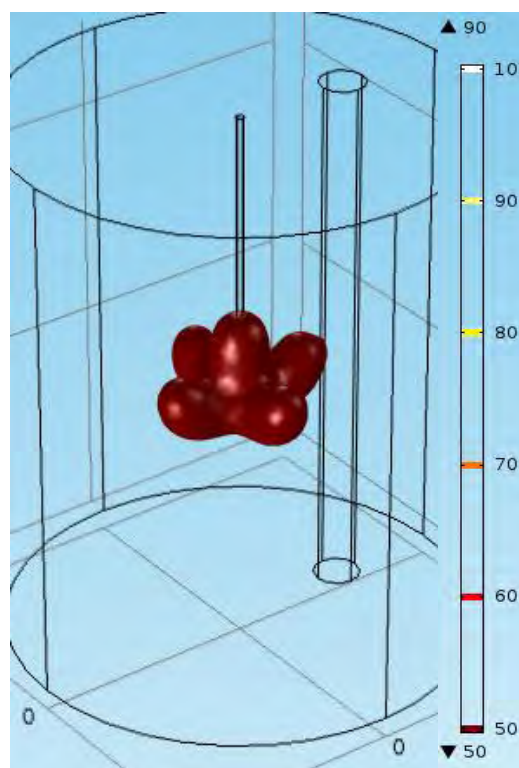
(i)



(ii)



(iii)



(iv)

Results and discussions

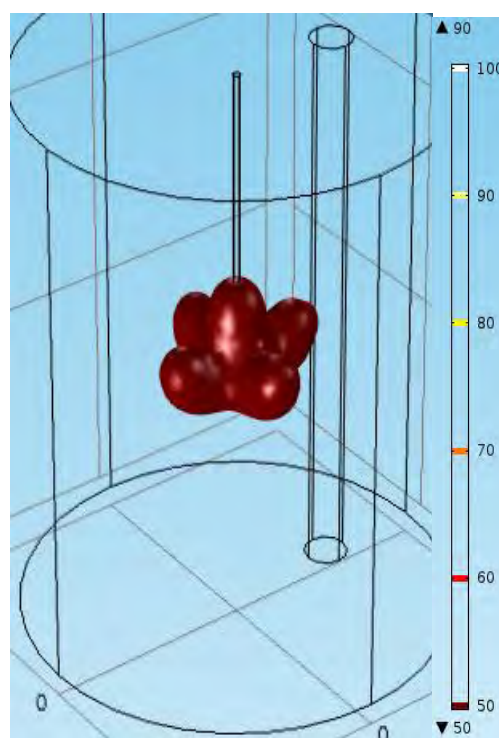
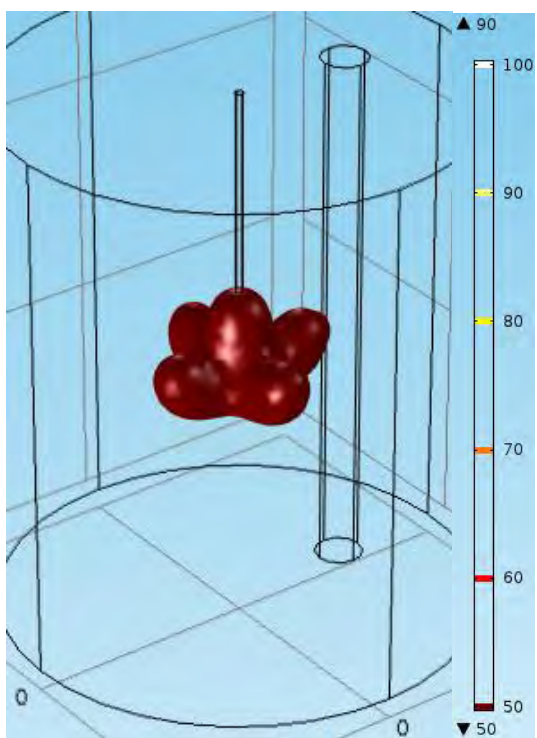
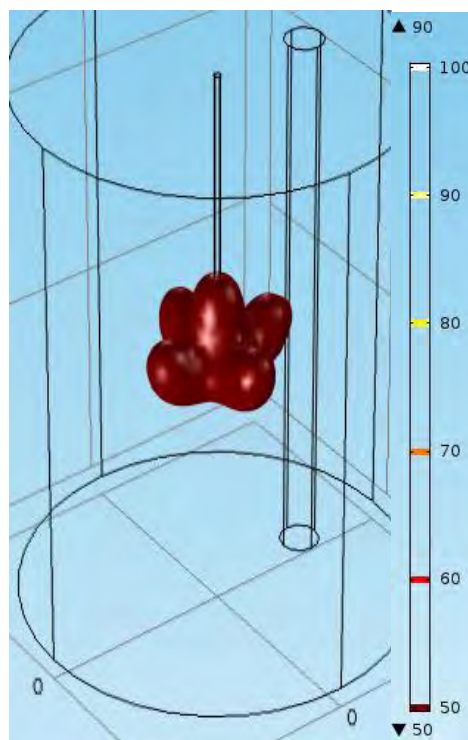
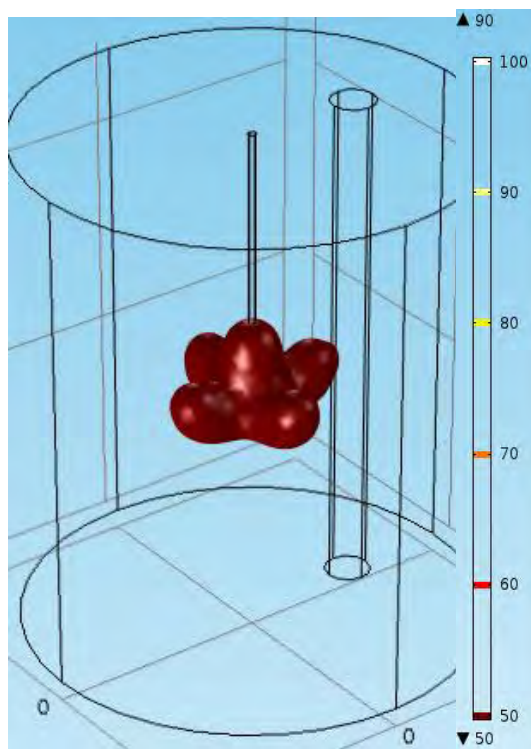
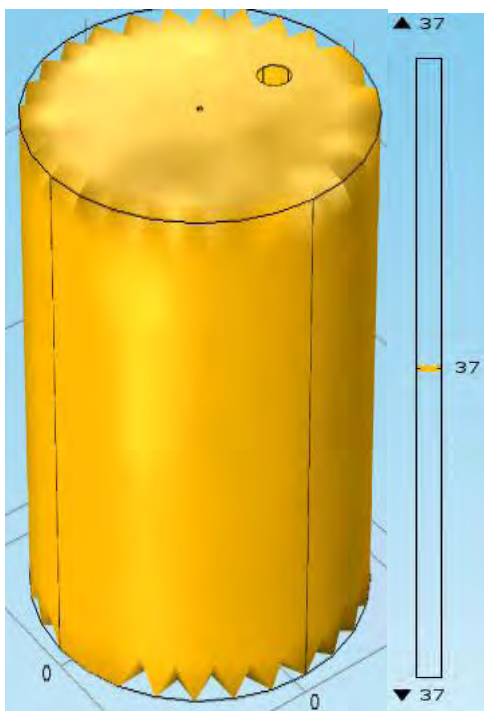
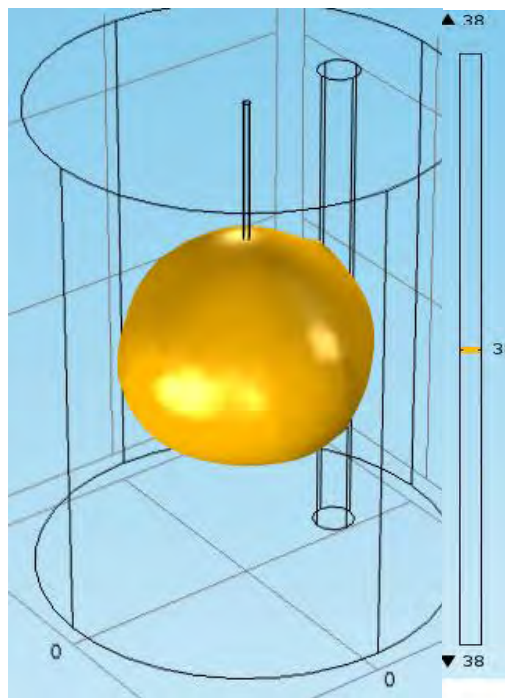


Figure 4.2: Iso-surfaces at 50°C for i) 60, ii) 120, iii) 180, iv) 240, v) 300, vi) 360, vii) 420 and viii) 480 s with 22V

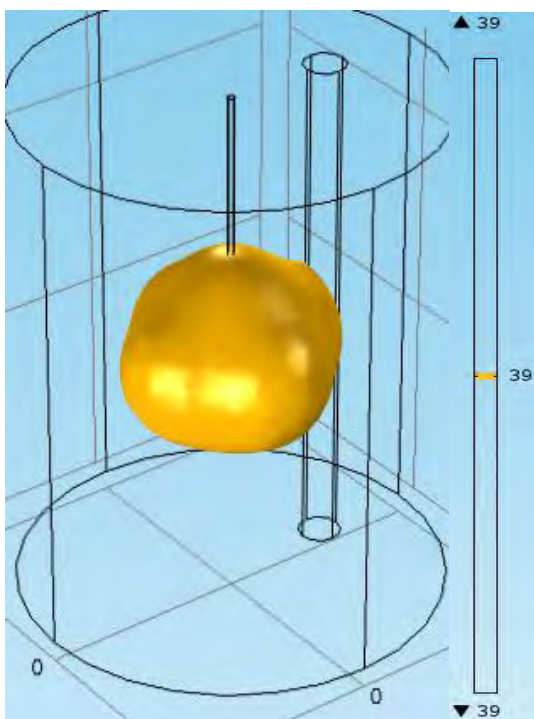
Results and discussions



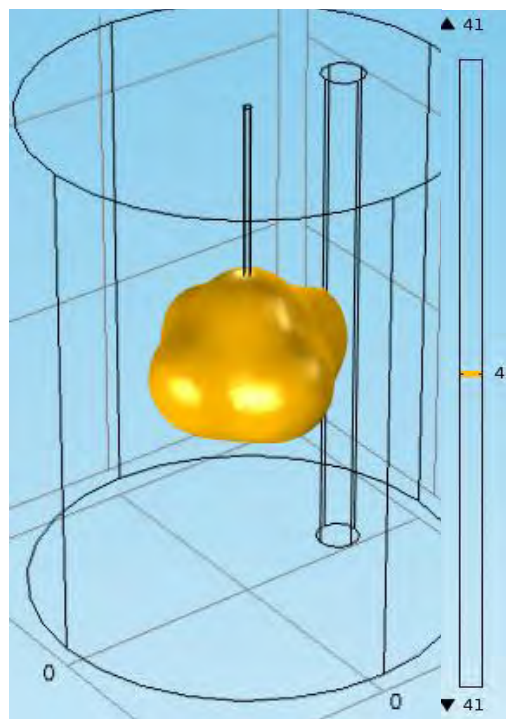
(i)



(ii)



(iii)



(iv)

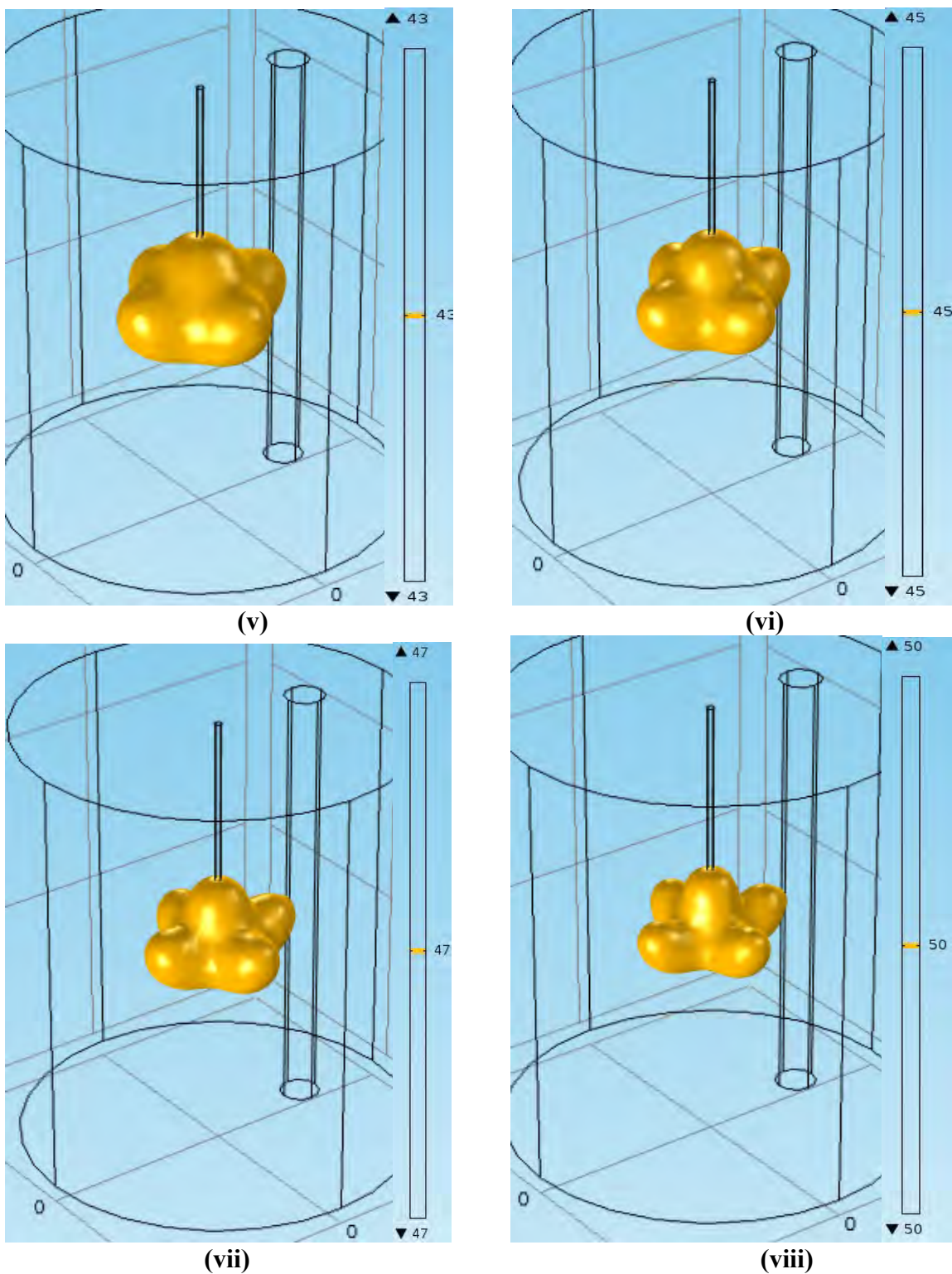


Figure 4.3: Iso-surfaces at (i) 37⁰C, (ii) 38⁰C, (iii) 39⁰C, (iv) 41⁰C, (v) 43⁰C, (vi) 45⁰C, (vii) 47⁰C and (viii) 50⁰C with 480 s and 22 V

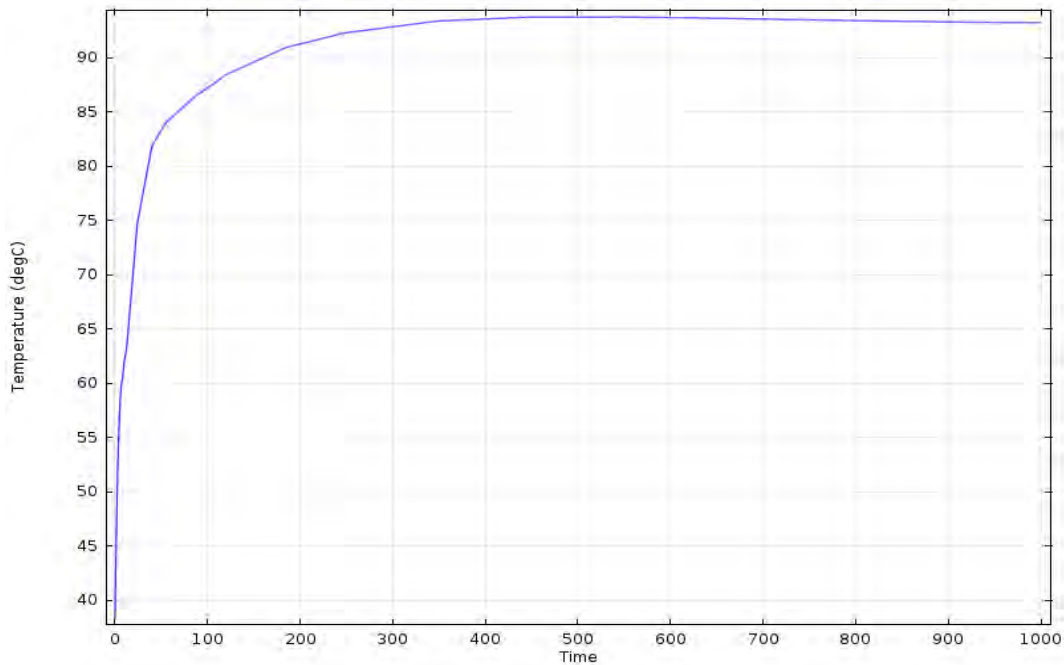


Figure 4.4: Temperature versus time at the tip of one of the electrodes arms at 22 V

4.3 Effect of Electric Voltage

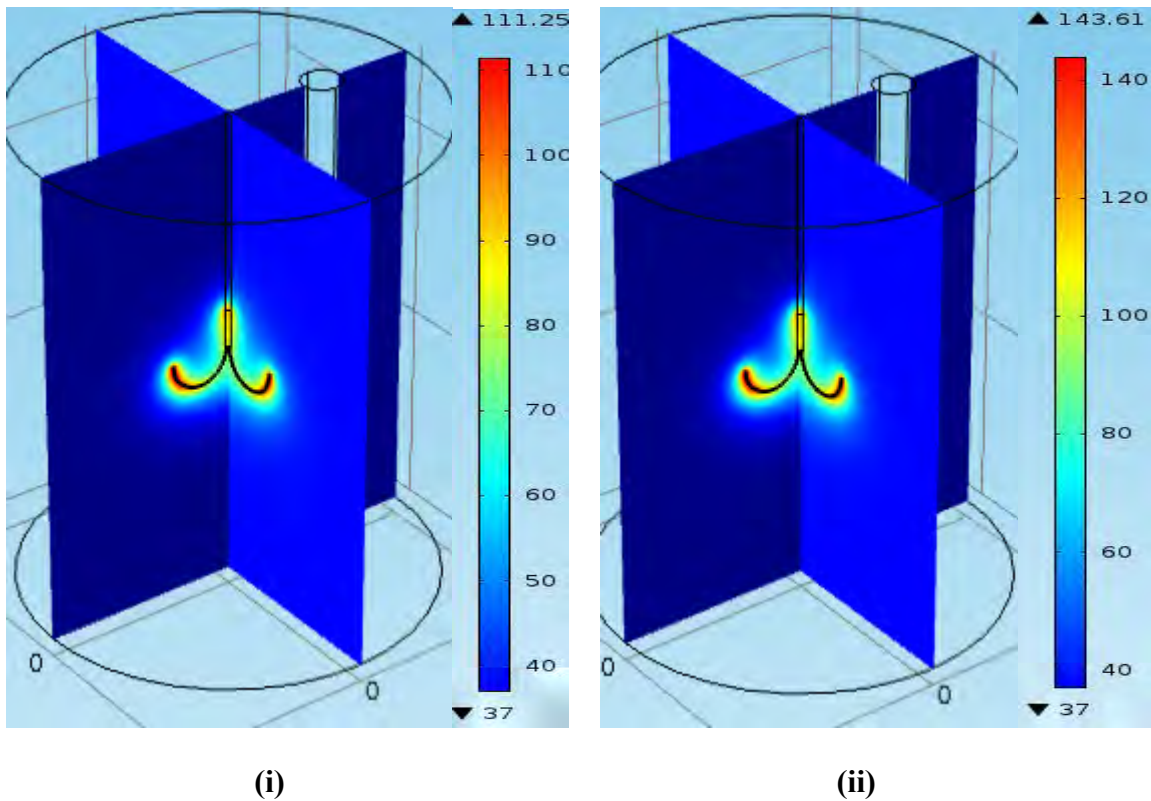
Figure 4.5 (i-vi) shows the temperature field at various electric voltages like 25, 30, 35, 40, 45, and 50 V at a fixed time of 480 s inside the tumor tissue. It has been seen that higher temperature exists at the central area of the liver whereas the tumor tissue locates. The electric current creates an electric field in the tissue through the probe. The probe generates resistive heating, which dominates around the probe's electrode arms because of the strong electric field. It can be seen that the temperature rises high when the electric voltage is high. Maximum temperature exists at the middle part of the tissue. The direction of the temperature increased in the cathode direction so that the tumor can be removed. There is a significant change in temperature due to the change of electric voltages. Here the changing color from blue to red represents lower to a higher temperature for all cases. Due to the increase in electric voltage, the temperature in the middle part of the tissue remains high and the area of this center part becomes hot in the surface plot.

Figure 4.6 (i-vi) shows the temperature versus time at the tip of one of the electrodes at various electric voltages like 25, 30, 35, 40, 45, and 50 V at a time from 0 to 600 s. It has shown that the changes of temperature with time at various voltage. The obtained temperature

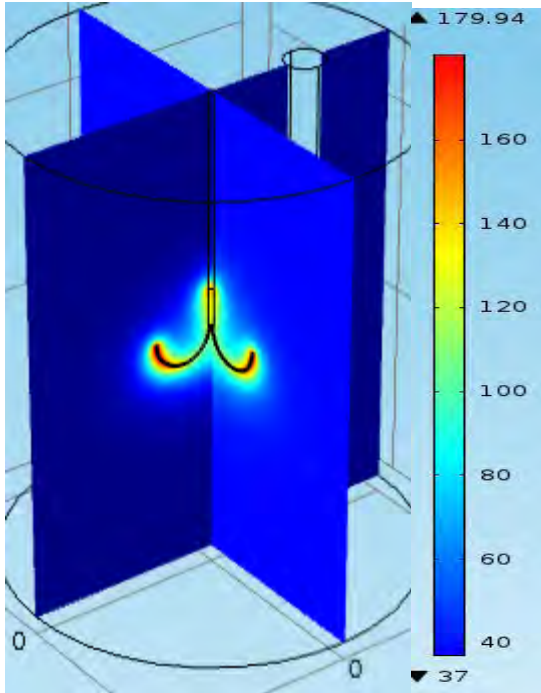
Results and discussions

at 25 V is lower than 50 V. Figure 4.6 shows the temperature versus time when the electric voltage changes, the lower number of electric voltages indicate the lower temperature. The results are determined by the electric voltages from 25 to 50 V when the temperature rises quickly until it reaches a steady-state temperature about 105, 130, 160, 200, 240, and 300°C respectively.

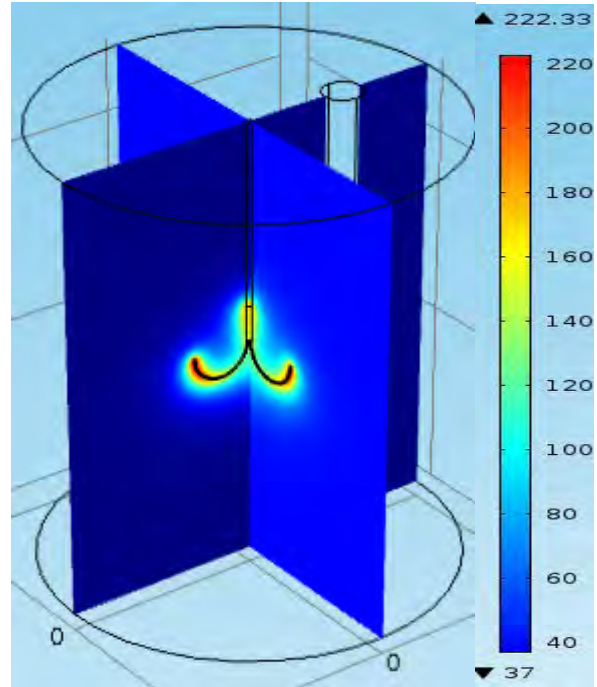
Figure 4.7 shows a point graph of the temperature versus time at the tip of one of the electrodes at various voltages from 25 to 50 V. It shows how the temperature increased with different electric voltages. The temperature rises due to increasing electric voltage.



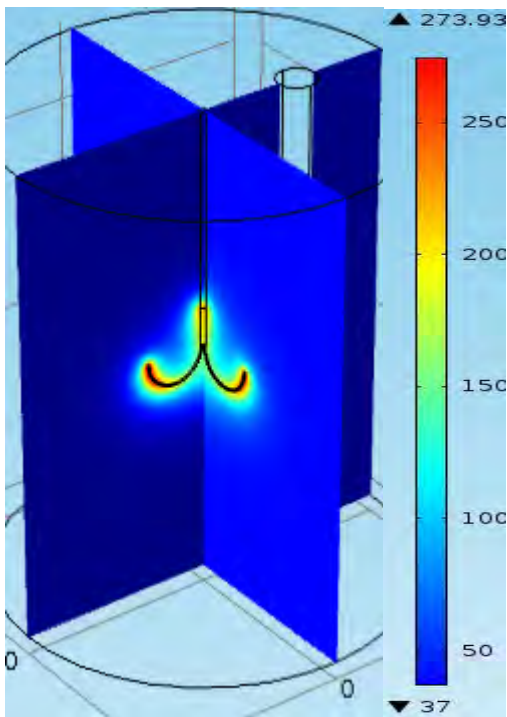
Results and discussions



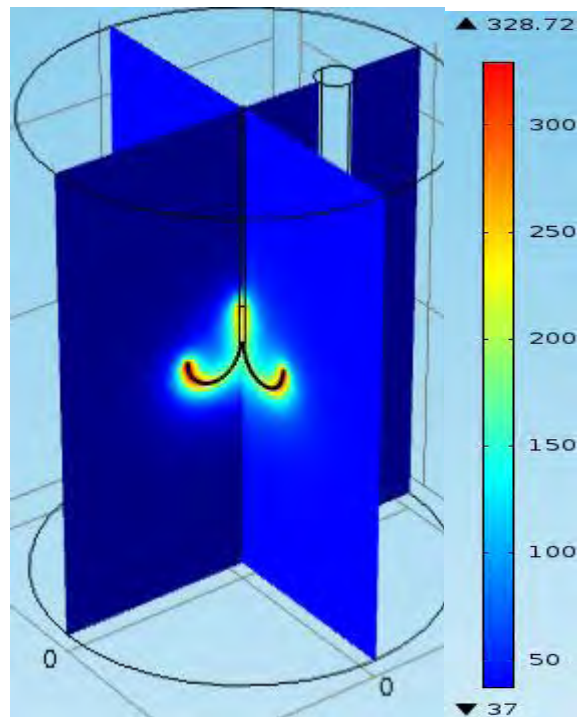
(iii)



(iv)



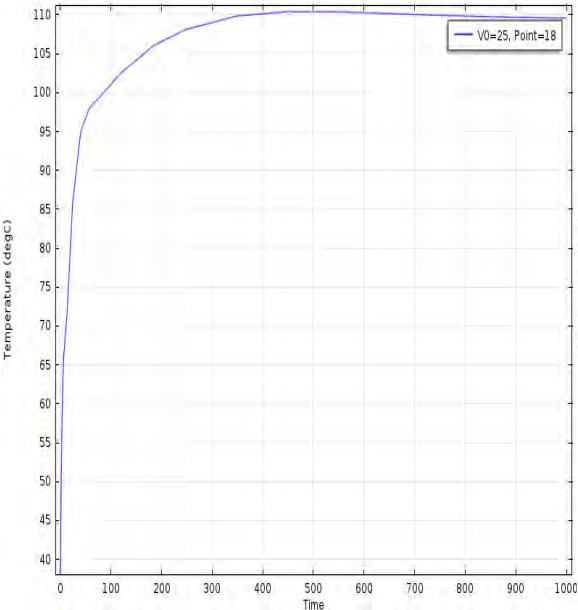
(v)



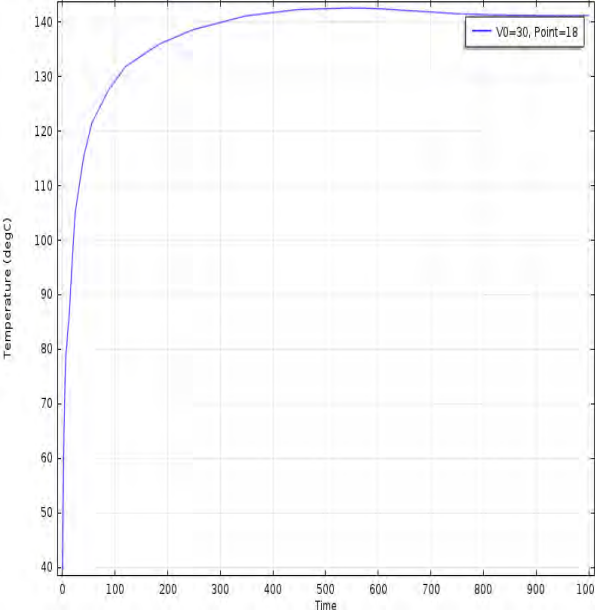
(vi)

Figure 4.5: Temperature fields at 480 s at various electric voltage i) 25, ii) 30, iii) 35, iv) 40, v) 45, vi) 50 V

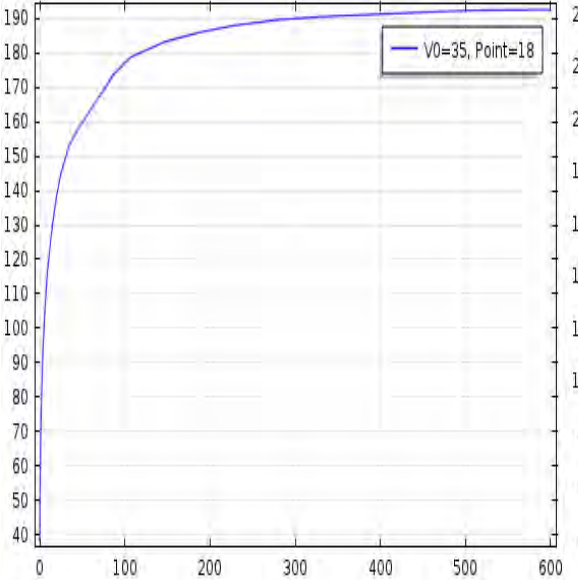
Results and discussions



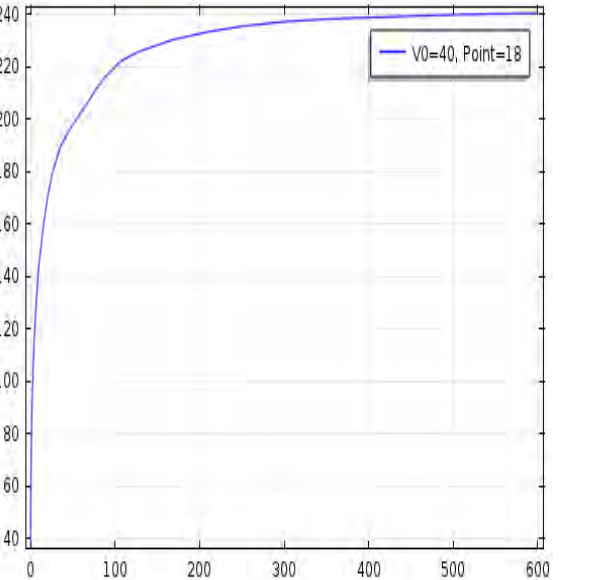
(i)



(ii)



(iii)



(iv)

Results and discussions

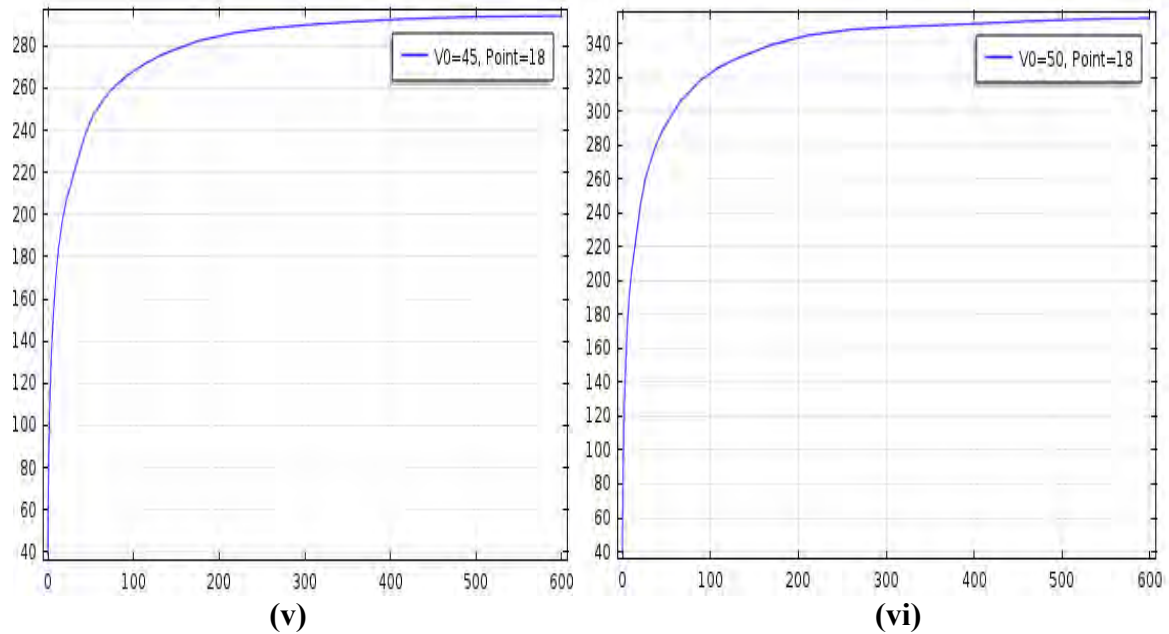


Figure 4.6: Temperature versus time at the tip of one of the electrode arms at i) 25, ii) 30, iii) 35, iv) 40, v) 45, and vi) 50 V.

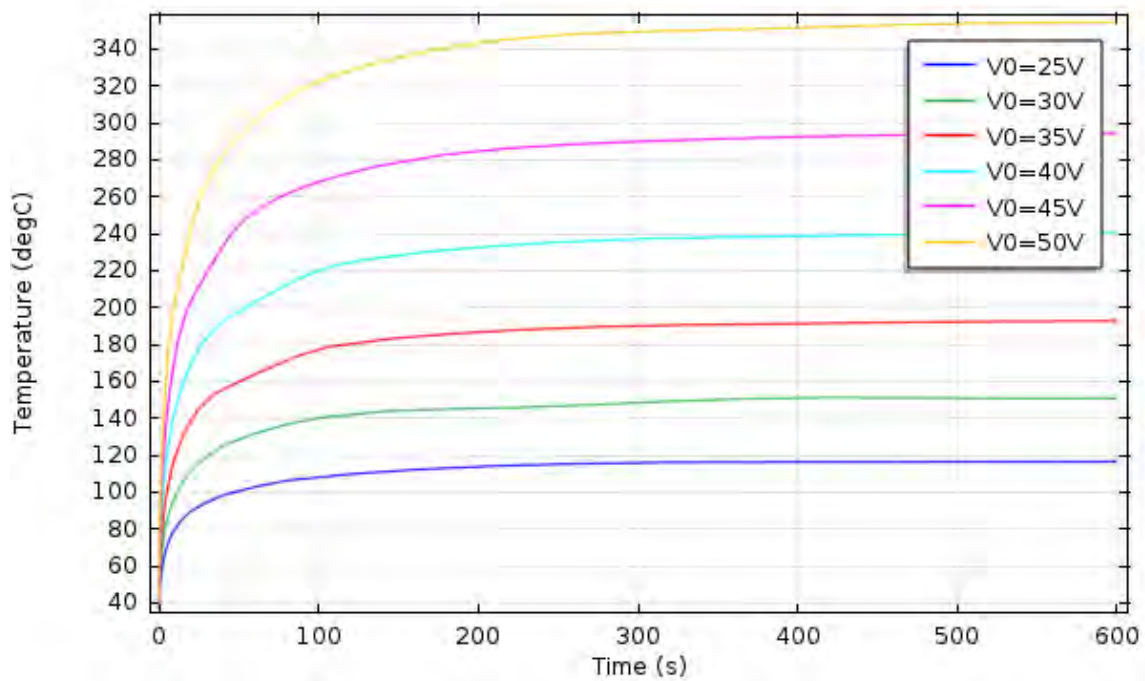


Figure 4.7: Temperature versus time at the tip of one of the electrodes from 25 to 50 V

4.4 Comparison

The obtained numerical results of the increasing temperature at the tip of the average one of the electrode directions among four-electrode arms at the point (16, 0, 50) mm with various times from the present study have been compared with that of Mellal *et al* [9]. They studied three-dimensional modeling using the finite element method for directional removal of a cancerous tumor. Mellal *et al* [9] used one arm electrode where we have used four-armed electrodes. The average applied power was 2 W in the model Mellal *et al* [9]. They had used AC current where we have used DC current in our model. They presented that the temperature increased in the cathode direction while remaining almost constant in the other directions in their paper. We observe that the increasing temperature is almost the same in the four cathode directions. That's why we have compared one of the cathodes which are located in the same direction as like cathode in the model of Mellal *et al*. [9]. Figure 4.8 depicts the comparative study of temperature for various times from 0 to 26 s with 30 V and 500 kHz.

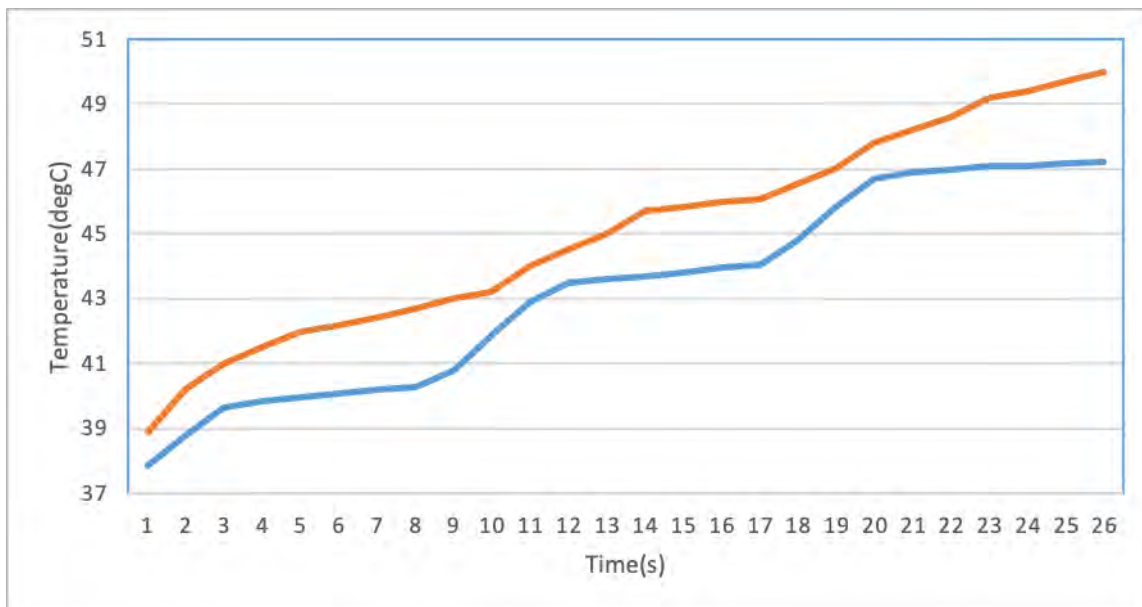


Figure 4.8: Comparison for temperature between Mellal *et al*. [9] (blue color) and present research (orange color)

The values of temperature for the same electrode of various times from the research of Mellal *et al*. [9] and the present research have been shown also in Table 4.1. Here the percentage of error between these two studies has also been included. This table also contains the percentage of error of the values between these two types of research. The minimum percentage of error,

Results and discussions

in this case, is 2.32 (approximately) at time 12 s. The maximum percentage of error (approximately 6.01%) occurs due to 8 s for which obtained values of temperature are 40.28⁰C and 42.70⁰C from the research of Mellal *et al.* [9] and the present research, respectively. A nice agreement is found in this comparison of results.

Table 4.1: Comparison of temperature between present numerical research and work of Mellal *et al.* [9]

Time (s)	Mellal <i>et al.</i> [9]	Present result	Percentage of error (%)	Time (s)	Mellal <i>et al.</i> [9]	Present result	Percentage of error (%)
1	37.86	38.90	2.75	14	43.70	45.69	4.55
2	38.77	40.20	3.69	15	43.82	45.84	4.61
3	39.64	41	3.43	16	43.96	45.99	4.62
4	39.83	41.50	4.19	17	44.05	46.07	4.59
5	39.97	42	5.08	18	44.81	46.54	3.86
6	40.08	42.20	5.29	19	45.81	47	2.60
7	40.21	42.40	5.45	20	46.71	47.80	2.33
8	40.28	42.70	6.01	21	46.88	48.20	2.82
9	40.80	43	5.39	22	46.97	48.60	3.47
10	41.86	43.20	3.20	23	47.10	49.20	4.46
11	42.88	44	2.61	24	47.11	49.40	4.86
12	43.49	44.50	2.32	25	47.16	49.70	5.39
13	43.59	45	3.23	26	47.21	50	5.91

CHAPTER 5

CONCLUSIONS AND FUTURE RESEARCH

Malignant tumors are cancerous. When cells grow uncontrollably, they develop. If the cells continue to grow and spread, the disease can become fatal. Malignant tumors move rapidly and imprint other parts of the process of metastasis. The cancer cells that move to other parts of the body are just like the original numbers and can invade other parts. If lung cancer spreads to the liver, liver cancer can happen.

A numerical study of controlling temperature through a four-armed electrode using Bioheat transfer equation and the electric current model has been conducted in the present research. Using Galerkin's weighted residual finite element technique, the governing equations have been solved. The effects of time and electric voltage in the form of temperature from 60 to 480 s on tumor tissue in the liver, Iso-surfaces at 50⁰C for various times with 22 V, Iso-surfaces from 37 to 50⁰C, and temperature versus time graph plot have been studied in detail. The effect of electric current has been observed from 25 to 50 V. Because of these arguments, the present study may be useful to remove a malignant tumor from the liver without destroying healthy tissue. From the present investigation the following conclusions may be drawn:

5.1 Conclusions

- A higher temperature of about 37 to 94⁰C is observed near the electrode and middle area of the tumor at different times from 60 to 480 s.
- Destruction of tumor tissue size increases by 50⁰C for increasing time from 60 to 480 s.
- Malignant tissue decreases approximately 100% due to increasing temperature from 37 to 50⁰C.
- The temperature of tumor tissue increases about 37 to 343⁰C with the increase of electric voltage from 22 to 50 V.
- The rising temperature reaches a steady-state temperature of about 90⁰C at 22 V.

Conclusions and recommendations

- Approximately 500 s time is needed to kill the tumor cell at 22 V.

5.2 Future Research

Future research can be done considering the following proposals:

- This research can be extended by including a blood vessel at a different distance from the malignant tissue of the liver.
- With technological advances in the design of radiofrequency ablation needles, the application of heat to tissues and the expansion of heat need to be intensively studied to overcome the imperfect proliferation of tumors due to the effects of vessel cooling and other radiofrequency ablation limitations.
- Together with more advanced interstitial imaging, such as CE-3DS, 3D navigation in laparoscopic radiofrequency ablation, radiofrequency ablation technology, and more refined histopathological assessment can be detected any complex liver tumor.
- In the future, the study can be extended by dissimilar physics like the electric voltage, power, impedance, and frequencies on malignant tissue.
- A comparative study between Microwave ablation and Radio-frequency ablation can be studied in the future.

REFERENCES

- [1] S. Tungitkusolmun, S.T. Staelin, D. Haemmerich, J.Z. Tsai, H. Cao, J.G. Webster, F.T. Lee, Jr. D.M. Mahvi and V.R. Vorperian, "Three-dimensional finite-element analyses for radio-frequency hepatic tumor ablation", IEEE Transactions On Biomedical Engineering, Vol. 49, No.1, pp. 3-8, 2002.
- [2] Z. Fang, B. Zhang, M. Moser, E. Zhang, and W. Zhang, "Design of a novel electrode of radiofrequency ablation for large tumor: a finite element study", Journal of Engineering and Science in Medical Diagnostics and Therapy, Vol. 1, pp. 011001, 2018.
- [3] B. Zhang, M.A.J. Moser, E.M. Zhang, Y. Luo, and W. Zhang, "Numerical analysis of the relationship between the area of target tissue necrosis and the size of target tissue in liver tumor with pulsed radiofrequency ablation", International Journal of Hyperthermia Vol. 31, No. 7, pp. 715-725, 2015.
- [4] R. Romero-Mendez and E. Berjano, "An analytical solution for radiofrequency ablation with a cooled cylindrical electrode", Mathematical Problems in Engineering, Vol. 2017, Article ID 9021616 1, pp. 1-12, 2017.
- [5] S.K. Hall, E.H. Ooi and S.J. Payne, "Cell death, perfusion, and electrical parameters are critical in models of hepatic radiofrequency ablation", Radio Graphics, Vol. 31, No. 5, pp. 538-550, 2015.
- [6] A.G. Suarez, F. Hornero and E.J. Berjano, "Mathematical modeling of epicardial RF ablation of atrial tissue with overlying epicardial fat", The Open Biomedical Engineering Journal, Vol. 4, pp. 47-55, 2010.
- [7] D. Haemmerich and B.J. Wood, "Hepatic radiofrequency ablation at low frequencies preferentially heat tumor tissue", International Journal of Hyperthermia, Vol. 22, No. 7, pp. 563-574, 2006.
- [8] E.M. Knavel, MD and C.L. Brace, "Tumor ablation: common modalities and general practices", NIH public Access, Vol. 16, No. 4, pp. 192-200, 2013.

References

- [9] I. Mellal, E. Kengne, K.E. Guemhioui, and A. Lakhssassi, “3D modeling using the finite element method for directional removal of a cancerous tumor”, *iMedPub Journals*, Vol. 5, No. 4:28, pp. 1-8, 2016.
- [10] C. Rossmann, M.A. McCrackin, K.E. Armeson, and D. Haemmerich, “Temperature-sensitive liposomes combined with thermal ablation: effects of duration and timing of heating in mathematical models and in vivo”, *PLOS ONE*, Vol. 12, pp. e0179131, 2017.
- [11] B. Al Sakree, F. Andre, C. Bernat, E. Connault, P. Opolon, R.V. Davalos, B. Rubinsky and L.M. Mir, “Tumor ablation with irreversible electroporation”, *PLOS ONE*, Vol. 2, pp. e1135, 2017.
- [12] K. Pillai, J. Akhter, T.C. Chua, M. Shehata, N. Alzahrani, I. Al-Alem, D.L. Morris, “Heat sink effect on tumor ablation Characteristics as observed in Monopolar radiofrequency, Bipolar radiofrequency and Microwave, using ex vivo calf liver model”, *www.md-journal.com*, Vol. 94, No. 9, pp. 1-10, 2015.
- [13] O.O. Adheyaju, H.M. Al-Angari, and A.V. Sahakian, “The optimization of needle electrode number and placement for irreversible electroporation of hepatocellular carcinoma”, *Radiol Oncol*, Vol. 46(2), pp. 126-135, 2012.
- [14] Q. Zhu, Y. Shen, A. Zhang, and L.X. Xu, “Numerical study of the influence of water evaporation on radiofrequency ablation”, *Biomedical Engineering Online*, Vol. 12, pp. 127, 2013.
- [15] C.K. Sung, H.B. Kim, J.H. Jung, K.Y. Baik, K.W. Moon, H.S. Kim, J.H. Yi, and J.H. Chung, “Historical and mathematical analysis of the irreversibly electroporated liver tissue”, *Technology and Cancer Research and Treatment*, Vol. 16(4), pp. 488-496, 2016.
- [16] E.J. Berjano, "Theoretical modeling for radiofrequency ablation: state-of-the-art and challenge for the future", *Biomedical Engineering Online*, Vol. 5, pp. 24, 2006.
- [17] Z. Liu, M. Ahmed, Y. Weinstein, M. Yi, R.L. Mahajan, and S.N. Goldberg, “Characterization of the RF ablation–induced „oven effect“: the importance of

References

- background Tissue thermal conductivity on tissue heating”, *International Journal of Hyperthermia*, Vol. 22, No. 4, pp. 327-342, 2006.
- [18] V. Ekstrand, H. Wiksell, I. Schultz, B. Sandstedt, S. Rotstein, and A. Eriksson, “Influence of electrical and thermal properties on RF ablation of breast cancer: is the tumour preferentially heated?”, *Biomedical Engineering Online*, Vol. 4, pp. 41, 2005.
- [19] T. Kroger, I. Altrogge, T. Preusser, L. Pereira, D. Schmidt, A. Weihusen and H.O. Peitgen, “Numerical simulation of radio frequency ablation with state dependent material parameters in three space dimensions”, *Springer, MICCAI 2006*, Vol. 4191, pp. 380-388, 2006.
- [20] A. Gasselhuber, M.R. Dreher, A. Negussie, B.J. Wood, F. Rattay, and D. Haemmerich, “Mathematical spatio-temporal model of drug delivery from low temperature sensitive liposomes during radiofrequency tumour ablation”, *International Journal of Hyperthermia*, Vol. 26, pp. 499-513, 2010.
- [21] M. Trujillo and E. Berjano, “Review of mathematical functions used to model the temperature dependence of electrical and thermal conductivities of biological tissue in radiofrequency ablation”, *International Journal of Hyperthermia*, Vol. 29, pp. 590-597, 2013.
- [22] S. Payne, R. Flanagan, M. Pollari, T. Alhonnoro, C. Bost, D. O’Neill, T. Peng, and P. Stiegler, "Image-based multi-scale modeling and validation of radio-frequency ablation in liver tumours", *Phil. Trans. R. Soc.*, Vol. 369, pp. 4233-54, 2011.
- [23] G. Mahlbacher, L.T. Curtis, J. Lowengurb and H.B. Frieboes, “Mathematical modeling of tumor-associated macrophage interactions with the cancer microenvironment”, *Journal for Immunotherapy of Cancer*, Vol. 6, pp. 1-17, 2018.
- [24] G. Shafirstein and Y. Feng, “The role of mathematical modeling in thermal medicine”, *International Journal of Hyperthermia*, Vol. 29, pp. 259-261, 2013.
- [25] Z. Wang, I. Aarya, M. Gueorguieva, D. Liu, H. Luo, L. Manfredi, L. Wang, D. McLean, S. Coleman, S. Brown and A. Cuschieri, “Image-based 3D modeling and validation of radiofrequency interstitial tumor ablation using a tissue-mimicking breast

References

- phantom”, *International Journal of Computer Assisted Radiology and Surgery*, Vol. 7, pp. 941-948, 2012.
- [26] D. Haemmerich and J.G. Webster, “Automatic control of finite element models for temperature-controlled radiofrequency ablation”, *Biomedical Engineering Online*, Vol. 4, pp. 42, 2005.
- [27] R. Nasrin, A. Hossain, and I. Zahan, “Blood flow analysis inside a stenotic artery using Power-Law fluid model”, *Research & Development in Material science*, Vol. 13(1), pp. 1360-1368, 2020.
- [28] M. Surita, A. Marwaha and S. Marwaha, “Finite element analysis for optimizing antenna for microwave coagulation therapy”, *Journal of Engineering Science and Technology*, Vol. 7(4), pp. 462-470, 2012.